

---

# CHAPTER 11

---

## LATERAL EARTH PRESSURE

### 11-1 THE LATERAL EARTH PRESSURE PROBLEM

Lateral earth pressure is a significant design element in a number of foundation engineering problems. Retaining and sheet-pile walls, both braced and unbraced excavations, grain in silo walls and bins, and earth or rock contacting tunnel walls and other underground structures require a quantitative estimate of the lateral pressure on a structural member for either a design or stability analysis.

The method of plastic equilibrium as defined by the Mohr rupture envelope of Figs. 2-24 and 11-1*a* is most generally used for estimating the lateral pressure from earth and other materials such as grain, coal, and ore. On occasion one may use the finite-element (of the elastic continuum) method but this has several distinct disadvantages for most routine design. The FEM has more application for estimating pressure on tunnel liners and large buried conduits than for most lateral pressure analyses.

Earth pressures are developed during soil displacements (or strains) but until the soil is on the verge of failure, as defined by the Mohr's rupture envelope (see Fig. 11-1*a*), the stresses are indeterminate. They are also somewhat indeterminate at rupture since it is difficult to produce a plastic equilibrium state in a soil mass everywhere simultaneously—most times it is a progressive event. Nevertheless, it is common practice to analyze rupture as an ideal state occurrence, both for convenience and from limitations on obtaining the necessary soil parameters with a high degree of reliability.

Referring to Fig. 11-1*a*, we see two circles that are common to point *A* and tangent to the rupture line. Both these circles represent a state of plastic equilibrium in plane strain. One of the other circles such as *EA* or *AF* would be a steady-state  $K_o$  condition depending on the overconsolidation ratio (OCR) defined by Eq. (2-13) (with discussion in Sec. 2-8).

### 11-2 ACTIVE EARTH PRESSURE

Active earth pressure refers to the plastic equilibrium state defined by rupture circle *AC* of Fig. 11-1*a*. This equilibrium state is obtained from Fig. 11-1*b* and *c* as follows. First apply

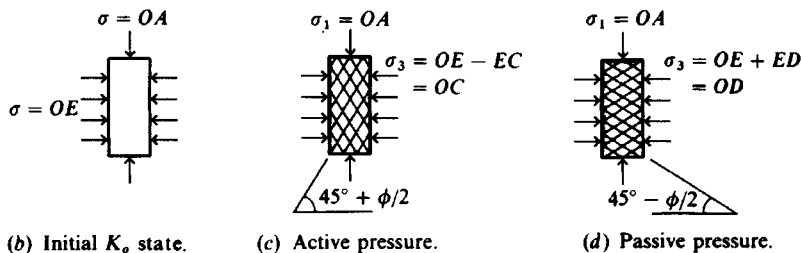
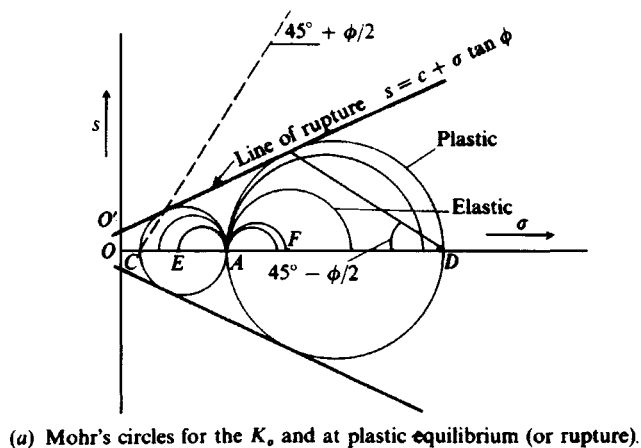


**Figure 11-1** Illustration of the concept of elastic and plastic equilibrium. Note in both (c) and (d) the slip lines are highly idealized. The stresses in (b), (c), and (d) such as  $OA$ ,  $OE$ ,  $EC$  are identified on the Mohr's circles of (a).

stresses  $OA$  and  $OE$  such that the initial  $K_0$  condition is obtained. Next gradually decrease  $OE$  to failure at  $OC$ . Stresses  $OA$  (maximum) and  $OC$  (minimum) can be used to plot a Mohr's circle. The difference between  $OA$  and  $OC$  is the circle diameter and is also the deviator stress as might be obtained in a laboratory  $CK_0UE$  triaxial test (see Fig. 2-40, case 2). The slip lines form as shown, since the horizontal and vertical planes defining the soil element in Fig. 11-1b are principal planes when the  $K_0$  state is developed. The latter is based on mechanics of materials and is independent of material; however, observations of model walls in sand indicates the slip-line angle of  $45^\circ + \phi/2$  shown is approximately developed.

The minimum principal stress  $OC = \sigma_3$  is termed the *active earth pressure* and can be computed using Eq. (2-55), repeated here for convenience:

$$\sigma_3 = \sigma_1 \tan^2 \left( 45^\circ - \frac{\phi}{2} \right) - 2c \tan \left( 45^\circ - \frac{\phi}{2} \right) \quad (2-55)$$

This equation was developed by Coulomb about 1776 in a considerably different form; Bell (1915) appears to be the first published source of the equation in the above form. This equation is often written in European literature with the following trigonometric relationships for the tangent function:

$$\tan^2 \left( 45^\circ - \frac{\phi}{2} \right) = \frac{1 - \sin \phi}{1 + \sin \phi} \quad \tan \left( 45^\circ - \frac{\phi}{2} \right) = \frac{1 - \sin \phi}{\cos \phi}$$

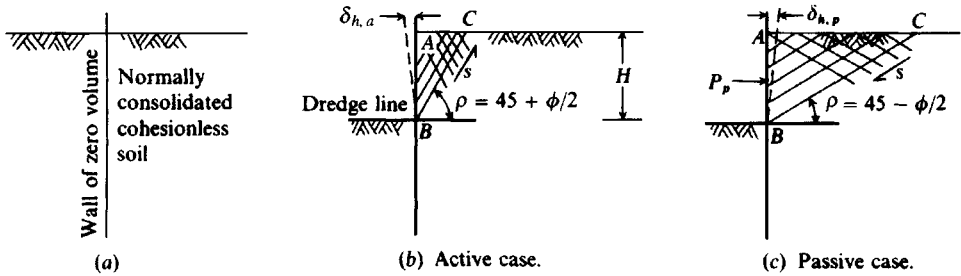


**Figure 11-2** Idealization of active and passive earth pressure from a  $K_o$  developed by inserting a wall of zero thickness (and volume) into a soil mass as in (a).

It is also usual to use  $K_a$  for the  $\tan^2$  term as shown previously in Fig. 4-2 and regularly used in this chapter. For the  $\tan(45^\circ + \phi/2)$  (passive) values of the next section, reverse the signs of the sine ratio terms.

Let us investigate the practical implications of Fig. 11-1 by using Fig. 11-2. In Fig. 11-2 we have inserted a wall of zero thickness into a normally consolidated; isotropic, cohesionless soil mass (we could use any soil but this simplifies the discussion). At this point we have a  $K_o$  stress state on the wall; and the lateral (soil-to-wall or wall-to-soil) pressure is, from the definition of  $K_o$ ,

$$\sigma_3 = K_o \sigma_1$$

and is triangular since at any depth  $z$  the vertical pressure  $\sigma_1 = \gamma z$ . If we assume the soil is normally consolidated,  $K_o$  can be defined by one of the qualitative stress ratios of Fig. 11-1a as

$$K_o = \frac{OE}{OA}$$

Now let us excavate the soil on the left side of the wall of Fig. 11-2a to the depth  $H$  in Fig. 11-2b and c. If the wall does not shear off at point  $B$  (termed the *dredge line*) the wall will do one of the following:

1. Deflect laterally under the cantilever beam loading causing slip planes to form in the soil as in Fig. 11-1c. The lateral pressure  $\sigma_h = \sigma_3$  on the Mohr's circle plot moves from  $E$  toward  $O$ . The Fig. 11-1c case develops since the  $K_o$  pressure exerted on the wall decreases as it deflects away from (but is followed by) the soil behind the wall.

If the wall displacement is sufficient, the lateral pressure reaches plastic equilibrium at  $OC$  and the wall pressure is a minimum (termed *active pressure case*) defined from Eq. (2-55) as

$$\sigma_h = \sigma_1 K_a \quad (\text{since } c = 0)$$

This minimum pressure case can be explained from observing that the slip wedge is a minimum volume at  $45^\circ + \phi/2$  from the horizontal. That is, the slope of the line from  $C$  to the point of tangency of Fig. 11-1a is also the slope of line  $BC$  of Fig. 11-2b. The shear resistance developed on line  $BC$  of Fig. 11-2b also reduces the tendency of the wedge  $ABC$  to push against the wall.

If the lateral displacement ( $\delta_{h,a}$ ) is limited (by a brace, prop, or wall stiffness), the wall pressure becomes indeterminate but is intermediate between the  $K_o$  and  $K_a$  pressures

(pressures  $OE$  and  $OC$  of Fig. 11-1a). The reason is that soil requires some limiting strain to mobilize the maximum shear resistance on the slip planes. This active pressure case is approximately illustrated as case 2 of Fig. 2-40 since Fig. 11-2b shows the wall rotating about the base  $B$ , whereas Fig. 2-40 shows a wall translation. Wall pressures depend on both wall movement and mode of movement.

2. Not deflect at all if the wall is sufficiently rigid and in this case the lateral pressure remains at

$$\sigma_h = \gamma z K_o$$

Since a lateral displacement of the wall produces a state of active earth pressure at the point where the wall pressure reduces to a minimum, we might ask what happens if there is no wall. In this case we have  $\sigma_3 = \sigma_h = 0$ , and it is evident that if the soil resistance mobilized on the slip plane (as  $BC$  of Fig. 11-2b) is not sufficient to satisfy statics of the wedge  $ABC$  the soil will slip into the excavation. This action can be readily observed in a small excavation in dry sand where the sides form slopes at some angle with the horizontal.

It should also be evident that as a hole is opened the surrounding soil will immediately displace laterally along similar slip planes into the cavity. When this shift happens, any device inserted into the hole must first "push" this displaced soil back to its original location before the in situ state is reproduced. It turns out that pushing the soil back to its original location is nearly impossible and, additionally, we introduce changes in the soil structure. This makes it very difficult to measure  $K_o$  in any excavated hole—including boreholes.

Since the wall must displace/rotate laterally away from the soil being retained to produce active (or  $K_a$ ) earth pressure conditions, the question is, how much rotation is necessary? This has been modestly investigated and the following may be used as a guide:

Soil and condition	Amount of translation, $\delta_{h,a}$
Cohesionless, dense	0.001 to 0.002H
Cohesionless, loose	0.002 to 0.004H
Cohesive, firm	0.01 to 0.02H
Cohesive, soft	0.02 to 0.05H

As previously stated, if there is not sufficient lateral displacement, the wall pressure is indeterminate between  $K_o$  and  $K_a$ . Most walls are designed for resisting active earth pressure since any rotation that tends to produce failure is usually large enough to allow the active (or minimum) pressure to develop. If the wall is rigid or if top rotation may be undesirable for aesthetic reasons, the wall is designed for higher (usually for  $K_o$ ) wall pressures. Even in this case if the wall starts into failure mode some rotation/translation will take place and the lateral pressure will start a reduction toward the  $K_a$  state. Failures of structural walls are most likely to occur during backfilling where compaction of the backfill with heavy rollers may induce a lateral pressure too large for the wall to support. Only in excavations do the conditions approximate Fig. 11-2a, b. In these cases the wall is usually installed then excavated to some depth. Lateral bracing is then installed and the excavation continued to another depth, bracing installed, etc. The lateral pressure retained by the wall should be at least  $K_o$  or somewhat larger; otherwise the ground around the excavation sinks and if structures are in the settling zone they crack and lawsuits result.

### 11-3 PASSIVE EARTH PRESSURE

The *passive earth pressure state* is given by the larger Mohr's circle of Fig. 11-1a. This state is developed by obtaining  $K_o$  conditions of Fig. 11-1b and holding  $OA$  constant while increasing the lateral pressure from  $OE$  to the plastic equilibrium failure at  $OD$  (and the case 4 situation of Fig. 2-40). The slip planes in the soil now make angles that are  $45^\circ - \phi/2$  with the horizontal and are  $\phi$  from the active state. This slip angle orientation is shown by the line from  $D$  to the point of tangency of the large Mohr's circle of Fig. 11-1a.

The major principal stress  $OD = \sigma_1$  can be computed from the geometry of Mohr's circle similarly as for the active pressure case to obtain Eq. (2-54) of Sec. 2-11:

$$\sigma_1 = \sigma_3 \tan^2 \left( 45^\circ + \frac{\phi}{2} \right) + 2c \tan \left( 45^\circ + \frac{\phi}{2} \right) \quad (2-54)$$

Passive earth pressure developed by increasing the lateral pressure from  $OE$  to  $OD$  of Fig. 11-1b and  $d$  is analogous to pushing the wall of Fig. 11-2c into the soil. Again the soil undergoes deformation and with sufficient deformation the maximum shear resistance is mobilized; however, note these points:

1. The resisting passive wedge volume is substantially larger.
2. The mobilized shear resistance  $s$  reverses direction to *increase* the wall force. The shear direction of the active case assists in reducing the wall force.

The change in the resisting wedge  $ABC$  of Figs. 11-2b, c is the principal reason why a wall that moves forward to the minimum active pressure case cannot be pushed back to its original position.

Figure 11-3 illustrates the relative movements and order of magnitude of the lateral earth pressure coefficients defined by the trigonometric ratios of Eqs. (2-54) and (2-55). Typically, passive earth pressure is developed by anchor plates or blocks embedded in the soil with a tension rod or cable oriented so that the cable pulls the block against the soil. Another case of passive pressure is the soil below the dredge line of Fig. 11-2, which must resist the wall

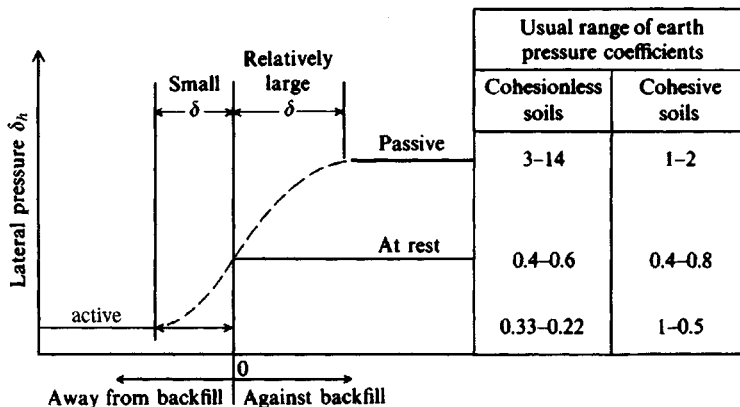


**Figure 11-3** Illustration of active and passive pressures with usual range of values for cohesionless and cohesive soil.

moving forward from point  $B$  down so that active pressure can develop behind the wall from the soil wedge defined by line  $BC$ .

This discussion has been theoretical to this point. We must now develop a means to apply these principles in a general way to evaluate what the earth pressure will be for specific applications. There are currently two general procedures for soil masses and a theory of elasticity method for loads on the soil mass that is to be resisted by the wall. These methods will be considered in the following several sections.

## 11-4 COULOMB EARTH PRESSURE THEORY

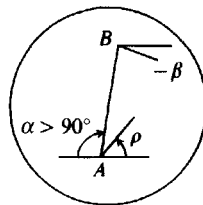
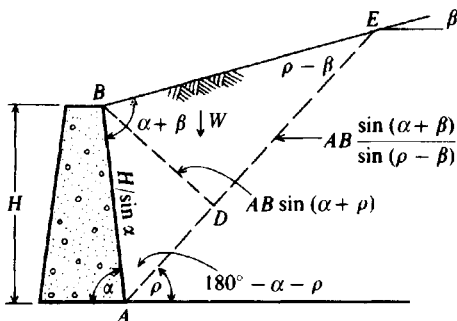
One of the earliest methods for estimating earth pressures against walls, credited to C. A. Coulomb (ca. 1776), made a number of assumptions as follows:

1. Soil is isotropic and homogeneous and has both internal friction and cohesion.
2. The rupture surface is a plane surface (as  $BC$  of Fig. 11-2b) and the backfill surface is planar (it may slope but is not irregularly shaped).
3. The friction resistance is distributed uniformly along the rupture surface and the soil-to-soil friction coefficient  $f = \tan \phi$ .
4. The failure wedge is a rigid body undergoing translation.
5. There is wall friction, i.e., as the failure wedge moves with respect to the back face of the wall a friction force develops between soil and wall. This friction angle is usually termed  $\delta$ .
6. Failure is a plane strain problem—that is, consider a unit interior slice from an infinitely long wall.

The principal deficiencies in the Coulomb theory are the assumptions that the soil is ideal and that the rupture zone is a plane (although for clean sand in the *active pressure* case, photographs of model walls indicate the rupture zone is very nearly a plane as  $BC$  of Fig. 11-2b).

The equations based on the Coulomb theory for a cohesionless soil can be derived from Figs. 11-4 and 11-5, using a large number of trigonometric relationships. The weight of the soil wedge  $ABE$ , for a unit thickness perpendicular to the drawing, of Fig. 11-4 is

$$W = \gamma A(1) = \frac{\gamma H^2}{2 \sin^2 \alpha} \left[ \sin(\alpha + \rho) \frac{\sin(\alpha + \beta)}{\sin(\rho - \beta)} \right] \quad (a)$$



$$\begin{aligned} \text{Area} &= \frac{1}{2} \overline{BD} (\overline{AE}) \\ \overline{AE} &= \frac{AB \sin(\alpha + \beta)}{\sin(\rho - \beta)} \\ \overline{BD} &= \frac{AB \sin(\alpha + \rho)}{\sin \rho} \\ AB &= \frac{H}{\sin \alpha} \end{aligned}$$

**Figure 11-4** Failure wedge used in deriving the Coulomb equation for active pressure. Note  $\beta$  may be  $\pm$  ( $-$  in inset) and  $0 < \alpha < 180^\circ$  ( $> 90^\circ$  in inset).

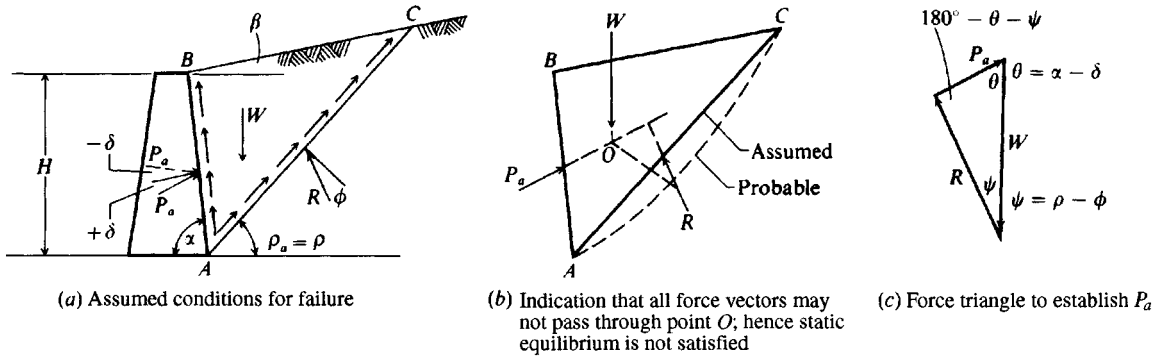


Figure 11-5 Coulomb active pressure wedge.

The active force  $P_a$  is a component of the weight vector as illustrated in Fig. 11-5c. Applying the law of sines, we obtain

$$\frac{P_a}{\sin(\rho - \phi)} = \frac{W}{\sin(180^\circ - \alpha - \rho + \phi + \delta)}$$

or

$$P_a = \frac{W \sin(\rho - \phi)}{\sin(180^\circ - \alpha - \rho + \phi + \delta)} \quad (b)$$

From Eq. (b) we see that the value of  $P_a$  depends on angle  $\rho$ ; that is, all other terms for a given problem are constant, and the value of  $P_a$  of primary interest is the largest possible value. Combining Eqs. (a) and (b), we obtain

$$P_a = \frac{\gamma H^2}{2 \sin^2 \alpha} \left[ \sin(\alpha + \rho) \frac{\sin(\alpha + \beta)}{\sin(\rho - \beta)} \right] \frac{\sin(\rho - \phi)}{\sin(180^\circ - \alpha - \rho + \phi + \delta)} \quad (c)$$

The maximum active wall force  $P_a$  is found from setting  $dP_a/d\rho = 0$  to give

$$P_a = \frac{\gamma H^2}{2} \frac{\sin^2(\alpha + \phi)}{\sin^2 \alpha \sin(\alpha - \delta) \left[ 1 + \sqrt{\frac{\sin(\phi + \delta) \sin(\phi - \beta)}{\sin(\alpha - \delta) \sin(\alpha + \beta)}} \right]^2} \quad (11-1)$$

If  $\beta = \delta = 0$  and  $\alpha = 90^\circ$  (a smooth vertical wall with horizontal backfill), Eq. (11-1) simplifies to

$$P_a = \frac{\gamma H^2}{2} \frac{(1 - \sin \phi)}{(1 + \sin \phi)} = \frac{\gamma H^2}{2} \tan^2 \left( 45^\circ - \frac{\phi}{2} \right) \quad (11-2)$$

which is also the Rankine equation for the active earth pressure considered in the next section. Equation (11-2) takes the general form

$$P_a = \frac{\gamma H^2}{2} K_a$$

where

$$K_a = \frac{\sin^2(\alpha + \phi)}{\sin^2 \alpha \sin(\alpha - \delta) \left[ 1 + \sqrt{\frac{\sin(\phi + \delta) \sin(\phi - \beta)}{\sin(\alpha - \delta) \sin(\alpha + \beta)}} \right]^2} \quad (11-3)$$

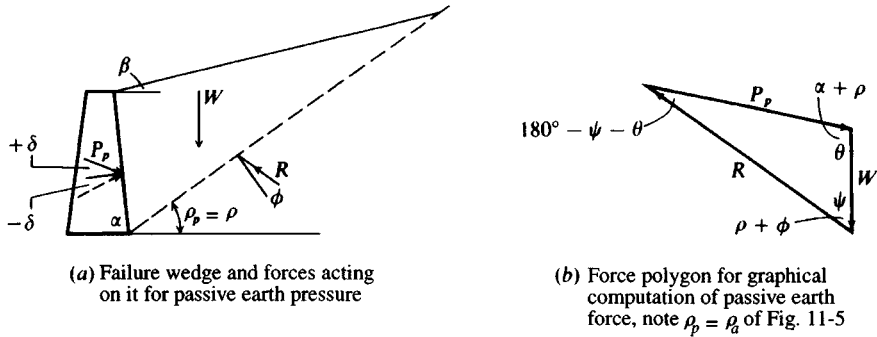


Figure 11-6 Coulomb passive pressure wedge.

and  $K_a$  is a coefficient that considers  $\alpha$ ,  $\beta$ ,  $\delta$ , and  $\phi$ , but is independent of  $\gamma$  and  $H$ . Table 11-1 gives values of  $K_a$  for selected angular values, and computer program FFACTOR on your diskette can be used to obtain values of  $K_a$  for other angle combinations.

Passive earth pressure is derived similarly except that the inclination at the wall and the force triangle will be as shown in Fig. 11-6.

From Fig. 11-6 the weight of the assumed failure mass is

$$W = \frac{\gamma H^2}{2} \sin(\alpha + \rho) \frac{\sin(\alpha + \beta)}{\sin(\rho - \beta)} \quad (d)$$

and from the force triangle, using the law of sines,

$$P_p = W \frac{\sin(\rho + \phi)}{\sin(180^\circ - \rho - \phi - \delta - \alpha)} \quad (e)$$

Setting the derivative  $dP_p/d\rho = 0$  gives the minimum value of  $P_p$  as

$$P_p = \frac{\gamma H^2}{2} \frac{\sin^2(\alpha - \phi)}{\sin^2 \alpha \sin(\alpha + \delta) \left[ 1 - \sqrt{\frac{\sin(\phi + \delta) \sin(\phi + \beta)}{\sin(\alpha + \delta) \sin(\alpha + \beta)}} \right]^2} \quad (11-4)$$

For a smooth vertical wall with horizontal backfill ( $\delta = \beta = 0$  and  $\alpha = 90^\circ$ ), Eq. (11-4) simplifies to

$$P_p = \frac{\gamma H^2}{2} \frac{1 + \sin \phi}{1 - \sin \phi} = \frac{\gamma H^2}{2} \tan^2 \left( 45^\circ + \frac{\phi}{2} \right) \quad (11-5)$$

Equation (11-4) can also be written

$$P_p = \frac{\gamma H^2}{2} K_p$$

where

$$K_p = \frac{\sin^2(\alpha - \phi)}{\sin^2 \alpha \sin(\alpha + \delta) \left[ 1 - \sqrt{\frac{\sin(\phi + \delta) \sin(\phi + \beta)}{\sin(\alpha + \delta) \sin(\alpha + \beta)}} \right]^2} \quad (11-6)$$

Table 11-2 gives values for  $K_p$  for selected angular values of  $\phi$ ,  $\alpha$ ,  $\delta$ , and  $\beta$ . Use program FFACTOR for other values and  $\alpha \neq 90^\circ$ .



TABLE 11-1

Coulomb active earth pressure coefficients  $K_a$  using Eq. (11-3)

		ALPHA = 90				BETA = -10			
$\delta$	$\phi = 26$	28	30	32	34	36	38	40	42
0	0.354	0.328	0.304	0.281	0.259	0.239	0.220	0.201	0.184
16	0.311	0.290	0.270	0.252	0.234	0.216	0.200	0.184	0.170
17	0.309	0.289	0.269	0.251	0.233	0.216	0.200	0.184	0.169
20	0.306	0.286	0.267	0.249	0.231	0.214	0.198	0.183	0.169
22	0.304	0.285	0.266	0.248	0.230	0.214	0.198	0.183	0.168
		ALPHA = 90				BETA = -5			
$\delta$	$\phi = 26$	28	30	32	34	36	38	40	42
0	0.371	0.343	0.318	0.293	0.270	0.249	0.228	0.209	0.191
16	0.328	0.306	0.284	0.264	0.245	0.226	0.209	0.192	0.176
17	0.327	0.305	0.283	0.263	0.244	0.226	0.208	0.192	0.176
20	0.324	0.302	0.281	0.261	0.242	0.224	0.207	0.191	0.175
22	0.322	0.301	0.280	0.260	0.242	0.224	0.207	0.191	0.175
		ALPHA = 90				BETA = 0			
$\delta$	$\phi = 26$	28	30	32	34	36	38	40	42
0	0.390	0.361	0.333	0.307	0.283	0.260	0.238	0.217	0.198
16	0.349	0.324	0.300	0.278	0.257	0.237	0.218	0.201	0.184
17	0.348	0.323	0.299	0.277	0.256	0.237	0.218	0.200	0.183
20	0.345	0.320	0.297	0.276	0.255	0.235	0.217	0.199	0.183
22	0.343	0.319	0.296	0.275	0.254	0.235	0.217	0.199	0.183
		ALPHA = 90				BETA = 5			
$\delta$	$\phi = 26$	28	30	32	34	36	38	40	42
0	0.414	0.382	0.352	0.323	0.297	0.272	0.249	0.227	0.206
16	0.373	0.345	0.319	0.295	0.272	0.250	0.229	0.210	0.192
17	0.372	0.344	0.318	0.294	0.271	0.249	0.229	0.210	0.192
20	0.370	0.342	0.316	0.292	0.270	0.248	0.228	0.209	0.191
22	0.369	0.341	0.316	0.292	0.269	0.248	0.228	0.209	0.191
		ALPHA = 90				BETA = 10			
$\delta$	$\phi = 26$	28	30	32	34	36	38	40	42
0	0.443	0.407	0.374	0.343	0.314	0.286	0.261	0.238	0.216
16	0.404	0.372	0.342	0.315	0.289	0.265	0.242	0.221	0.201
17	0.404	0.371	0.342	0.314	0.288	0.264	0.242	0.221	0.201
20	0.402	0.370	0.340	0.313	0.287	0.263	0.241	0.220	0.201
22	0.401	0.369	0.340	0.312	0.287	0.263	0.241	0.220	0.201
		ALPHA = 90				BETA = 15			
$\delta$	$\phi = 26$	28	30	32	34	36	38	40	42
0	0.482	0.440	0.402	0.367	0.334	0.304	0.276	0.251	0.227
16	0.447	0.408	0.372	0.340	0.310	0.283	0.258	0.234	0.213
17	0.447	0.407	0.372	0.339	0.310	0.282	0.257	0.234	0.212
20	0.446	0.406	0.371	0.338	0.309	0.282	0.257	0.234	0.212
22	0.446	0.406	0.371	0.338	0.309	0.282	0.257	0.234	0.212

TABLE 11-2

Coulomb passive earth pressure coefficients  $K_p$  using Eq. (11-6)

		ALPHA = 90				BETA = -10				
$\delta$	$\phi =$	26	28	30	32	34	36	38	40	42
0		1.914	2.053	2.204	2.369	2.547	2.743	2.957	3.193	3.452
16		2.693	2.956	3.247	3.571	3.934	4.344	4.807	5.335	5.940
17		2.760	3.034	3.339	3.679	4.062	4.493	4.983	5.543	6.187
20		2.980	3.294	3.645	4.041	4.488	4.997	5.581	6.255	7.039
22		3.145	3.490	3.878	4.317	4.816	5.389	6.050	6.819	7.720

		ALPHA = 90				BETA = -5				
$\delta$	$\phi =$	26	28	30	32	34	36	38	40	42
0		2.223	2.392	2.577	2.781	3.004	3.250	3.523	3.826	4.163
16		3.367	3.709	4.094	4.529	5.024	5.591	6.243	7.000	7.883
17		3.469	3.828	4.234	4.694	5.218	5.820	6.516	7.326	8.277
20		3.806	4.226	4.704	5.250	5.879	6.609	7.462	8.468	9.665
22		4.064	4.532	5.067	5.684	6.399	7.236	8.222	9.397	10.809

		ALPHA = 90				BETA = 0				
$\delta$	$\phi =$	26	28	30	32	34	36	38	40	42
0		2.561	2.770	3.000	3.255	3.537	3.852	4.204	4.599	5.045
16		4.195	4.652	5.174	5.775	6.469	7.279	8.229	9.356	10.704
17		4.346	4.830	5.385	6.025	6.767	7.636	8.661	9.882	11.351
20		4.857	5.436	6.105	6.886	7.804	8.892	10.194	11.771	13.705
22		5.253	5.910	6.675	7.574	8.641	9.919	11.466	13.364	15.726

		ALPHA = 90				BETA = 5				
$\delta$	$\phi =$	26	28	30	32	34	36	38	40	42
0		2.943	3.203	3.492	3.815	4.177	4.585	5.046	5.572	6.173
16		5.250	5.878	6.609	7.464	8.474	9.678	11.128	12.894	15.076
17		5.475	6.146	6.929	7.850	8.942	10.251	11.836	13.781	16.201
20		6.249	7.074	8.049	9.212	10.613	12.321	14.433	17.083	20.468
22		6.864	7.820	8.960	10.334	12.011	14.083	16.685	20.011	24.352

		ALPHA = 90				BETA = 10				
$\delta$	$\phi =$	26	28	30	32	34	36	38	40	42
0		3.385	3.712	4.080	4.496	4.968	5.507	6.125	6.840	7.673
16		6.652	7.545	8.605	9.876	11.417	13.309	15.665	18.647	22.497
17		6.992	7.956	9.105	10.492	12.183	14.274	16.899	20.254	24.633
20		8.186	9.414	10.903	12.733	15.014	17.903	21.636	26.569	33.270
22		9.164	10.625	12.421	14.659	17.497	21.164	26.012	32.601	41.863

		ALPHA = 90				BETA = 15				
$\delta$	$\phi =$	26	28	30	32	34	36	38	40	42
0		3.913	4.331	4.807	5.352	5.980	6.710	7.563	8.570	9.768
16		8.611	9.936	11.555	13.557	16.073	19.291	23.494	29.123	36.894
17		9.139	10.590	12.373	14.595	17.413	21.054	25.867	32.409	41.603
20		11.049	12.986	15.422	18.541	22.617	28.080	35.629	46.458	62.759
22		12.676	15.067	18.130	22.136	27.506	34.930	45.584	61.626	87.354

Figure 11-1 displays that earth pressure is dependent on the *effective* stresses in the soil and not total stresses. It necessarily follows that the wall pressure below the water table is the sum of the hydrostatic pressure and the *effective* lateral earth pressure from using the *effective* unit weight  $\gamma'$  of the soil.

**Example 11-1.** What is the total active force per meter of wall for the soil-wall system, shown in Fig. E11-1, using the Coulomb equations? Where does  $P_a$  act?

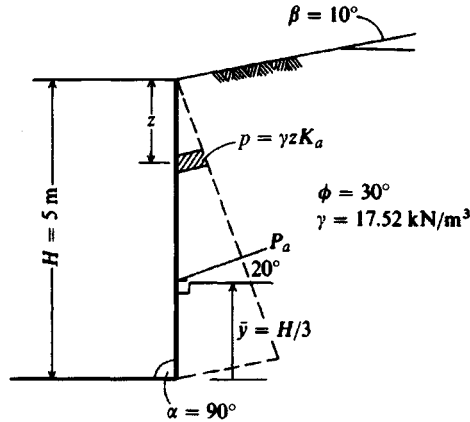


Figure E11-1

**Solution.** Take the wall friction  $\delta = 2\phi/3 = 20^\circ$  (a common estimate). For  $\phi = 30^\circ$  obtain  $K_a = 0.34$  from Table 11-1:

$$p_a = \gamma z K_a$$

$$P_a = \int_0^H \gamma z K_a dz = \frac{1}{2} \gamma H^2 K_a$$

$$P_a = \frac{1}{2} (17.52)(5)^2 (0.34) = 74.5 \text{ kN/m}$$

Summing moments about the top, we have

$$P_a \bar{y}' = \int_0^H \gamma z K_a z dz = \frac{\gamma H^3}{3} K_a$$

Using the symbolic  $P_a$  and equating, we obtain

$$\bar{y}' = \frac{2\gamma H^3 K_a}{3\gamma H^2 K_a} = \frac{2}{3} H \quad \text{from top or}$$

$$\bar{y} = H - \frac{2H}{3} = \frac{H}{3} \quad \text{from bottom (value usually used)}$$

For  $\delta = 20^\circ$  a force polygon would show that  $P_a$  will act on the wall as shown in Fig. E11-1.

////

**Example 11-2.** What is the total active force/unit width of wall and what is the location of the resultant for the system shown in Fig. E11-2a? Use the Coulomb equations and take a smooth wall so  $\delta = 0^\circ$ .

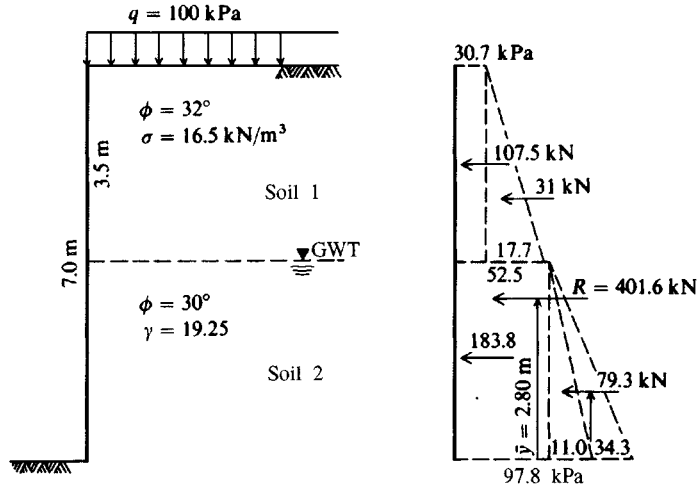


Figure E11-2

**Solution.** We have a surcharge, which is seen by the wall at  $z = 0$  as a pressure  $q$  (which could be caused by a fictitious soil depth of  $\gamma z_o$ ). There will be  $K_a$  values for each soil of

$$K_{a1} = 0.307 \quad K_{a2} = 0.333 \quad (\text{Table 11-1 and } \alpha = 90^\circ)$$

At  $z = 0$  (top of wall where surcharge acts) we have

$$p_1 = \gamma z_o K_a = q K_a = 100(0.307) = 30.7 \text{ kPa}$$

At the interface (interpreted as  $z - dz$ ) of top stratum  $z_1 = 3.5$  m and noting the surcharge  $q$  carries through to give the effect of  $q_z = \gamma z_o + \gamma z_1$ , we have

$$\begin{aligned} p_2 &= (q + \gamma z_1) K_a = [100 + 16.5(3.5)] 0.307 \\ &= 30.7 + 17.7 = 48.4 \text{ kPa} \end{aligned}$$

It is often convenient to retain the several effects separately. Here we see that  $q$  gives a rectangular (constant) wall pressure whereas the increasing depth of soil gives a triangular pressure diagram with 17.7 kPa at the base.

Continuing for soil 2, at depth  $z + dz = 3.5$  m we are into soil 2 and since that is the location of the water table we will have to use  $\gamma' = 19.25 - 9.81 = 9.44 \text{ kN/m}^3$ .

Just at the interface we have

$$\begin{aligned} p'_2 &= [q + 16.5(3.5) + 9.44 dz] K_{a2} \\ &= [100 + 16.5(3.5) + 0] 0.333 = 52.5 \text{ kPa} \end{aligned}$$

Note we have an abrupt discontinuity in the pressure diagram of 48.4 kPa and at  $3.5 + dx$  a pressure of 52.5 kPa. At the bottom of the wall we have

$$p_3 = [100 + 16.5(3.5) + 9.44(3.5)] K_{a2}$$

which is the same as

$$\begin{aligned} p_3 &= 52.5 + 9.44(3.5) 0.333 \\ &= 52.5 + 11.0 = 63.5 \text{ kPa} \quad (\text{again the 11.0 is a triangle}) \end{aligned}$$

The water also contributes lateral pressure and has  $K_a = K_p = 1$  since  $\phi_w = 0^\circ$ . Thus,

$$p_w = \gamma_w z_w = 9.807(3.5) = \mathbf{34.3 \text{ kPa}}$$

These pressure values are plotted on Fig. E11-2b so the several pressure areas can be numerically integrated to obtain the total wall force. By using triangles and rectangles as shown, the total wall force is the sum from the several areas and the forces act through the centroids of the areas as shown so that we can easily sum moments about the base to obtain

$$R\bar{y} = \sum P_i y_i$$

$$P_1 = 30.7(3.5) = 107.5 \text{ kN} \quad y_i = 3.5 + \frac{3.5}{2} = 5.25 \text{ m}$$

$$P_2 = 17.7\left(\frac{3.5}{2}\right) = 31.0 \text{ kN} \quad y_2 = 3.5 + \frac{3.5}{3} = 4.67 \text{ m}$$

$$P_3 = 52.5(3.5) = 183.8 \text{ kN} \quad y_3 = \frac{3.5}{2} = 1.75 \text{ m}$$

Include water with  $P_4$  since both areas are triangles:

$$P_4 = (34.3 + 11.0)\left(\frac{3.5}{2}\right) = 79.3 \text{ kN} \quad y_4 = \frac{3.5}{3} = 1.17$$

$$R = \sum P_i = 107.5 + 31.0 + 183.8 + 79.3 = \mathbf{401.6 \text{ kN}}$$

Now sum the moments for  $\bar{y}$ :

$$401.6\bar{y} = 107.5(5.25) + 31.0(4.67) + 183.8(1.75) + 79.3(1.17)$$

$$\bar{y} = \frac{1123.6}{401.6} = \mathbf{2.80 \text{ m}} \quad (\text{above wall base})$$

////

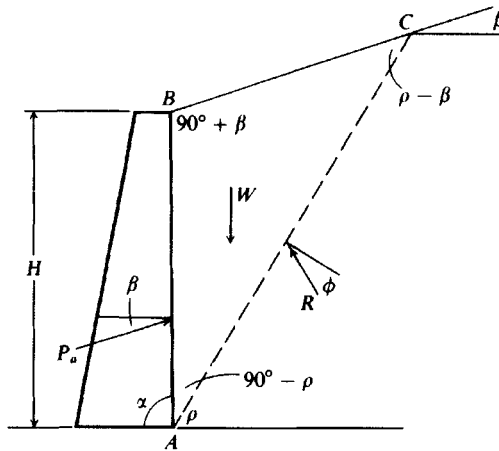
## 11-5 RANKINE EARTH PRESSURES

Rankine (ca. 1857) considered soil in a state of plastic equilibrium and used essentially the same assumptions as Coulomb, except that *he assumed no wall friction or soil cohesion*. The Rankine case is illustrated in Fig. 11-7 with a Mohr's construction for the general case shown in Fig. 11-8. From Fig. 11-8 we can develop the Rankine active and passive pressure cases by making substitution of the equation for  $r$  (shown on the figure) into the equations for  $EF$  (and  $FG$ ) (also shown on the figure). Then substitution into the expression for  $K'_a$  (with  $OB$  canceling and using  $\sin^2 \beta = 1 - \cos^2 \beta$ ) gives the pressure ratio acting parallel to backfill slope  $\beta$  as

$$K'_a = \frac{\cos \beta - \sqrt{\cos^2 \beta - \cos^2 \phi}}{\cos \beta + \sqrt{\cos^2 \beta - \cos^2 \phi}} \quad (11-7)$$

We note that the *horizontal component* of active earth pressure is obtained as

$$\sigma_{a,\text{hor}} = \sigma_a \cos \beta \quad (= OE \cos \beta = OA \text{ of Fig. 11-8b})$$

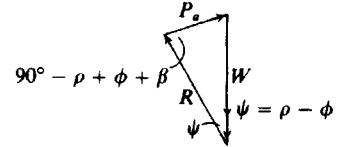


(a) Soil-structure system for the Rankine solution for  $\alpha = 90^\circ$

$$\text{Area } ABC = \frac{1}{2} H^2 \frac{\sin(90^\circ - \rho) \sin(90^\circ + \beta)}{\sin(\rho - \beta)}$$

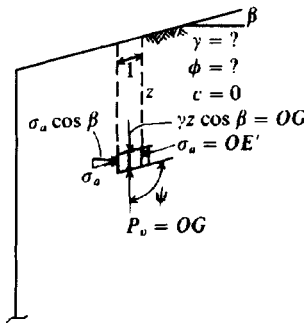
$$(1) W = \frac{1}{2} \gamma H^2 \frac{\cos \rho \cos \beta}{\sin(\rho - \beta)}$$

$$(2) P_a = W \frac{\sin(\rho - \phi)}{\sin(90^\circ - \rho + \phi + \beta)}$$

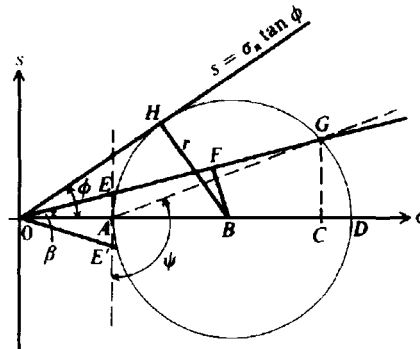


(b) Force triangle in the Rankine solution

Figure 11-7 Rankine active earth pressure wedge.



(a) General case: only for  $+\beta$  as shown.



(b) Mohr's circle.

$$OG = \gamma z \cos \beta$$

$$K'_a = \frac{OE}{OG} = \frac{OF - EF}{OF + FG} = \frac{OE'}{OG}$$

$$K'_p = \frac{OF + FG}{OF - EF}$$

$$OF = OB \cos \beta$$

$$\text{Since } BF \text{ bisects } EG,$$

$$EF = FG = \sqrt{r^2 - BF^2}$$

$$BF = OB \sin \beta$$

$$r = OB \sin \phi$$

Figure 11-8 General conditions and Mohr's circle to derive the Rankine earth pressure equations.

By analogy (and referring again to Fig. 11-8) we obtain the pressure ratio for  $K'_p$  in a similar manner:

$$K'_p = \frac{\cos \beta + \sqrt{\cos^2 \beta - \cos^2 \phi}}{\cos \beta - \sqrt{\cos^2 \beta - \cos^2 \phi}} \quad (11-8)$$

Noting that the ratio of  $K'_a = \sigma_a / (\gamma z \cos \beta)$  is for an earth pressure parallel to  $\beta$  and that the vertical pressure on a horizontal plane at depth  $z$  is  $\gamma z \cos \beta$ , we have

$$\sigma_a = \gamma z \cos \beta K'_a$$



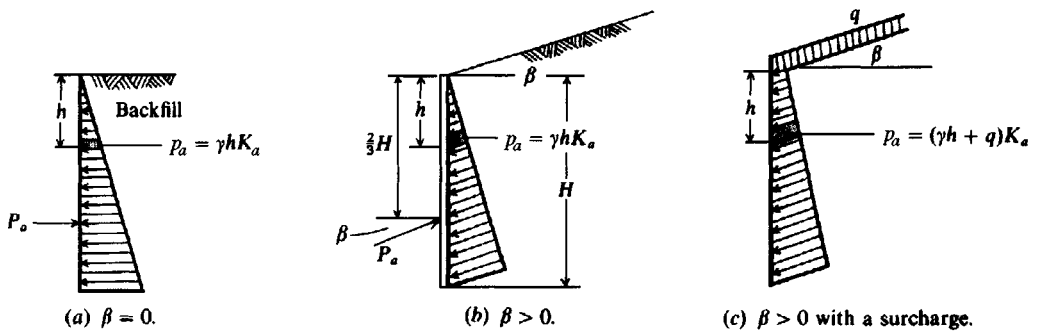


Figure 11-9 Rankine active earth pressure diagrams in a cohesionless soil.

**Example 11-3.** What is the total active earth force per meter of wall for the wall system shown in Example 11-1 using the Rankine equation?

**Solution.** For  $\beta = 10^\circ$  and  $\phi = 30^\circ$  we obtain  $K_a = 0.3495$  from Table 11-3. Directly substituting into Eq. (11-9), we may write

$$P_a = \frac{1}{2} \gamma H^2 K_a = \frac{1}{2} (17.52)(5)^2 0.350 = 76.6 \text{ kN/m}$$

This value compares with 74.5 kN/m by the Coulomb equation, for a difference of about 2 percent, but acts here at a wall angle of  $\beta = \delta = 10^\circ$  as shown on Fig. E11-3 instead of  $\delta = 20^\circ$  of Fig. E11-1. The horizontal and vertical force components are

$$P_{a,h} = P_a \cos 10^\circ = 76.6 \cos 10^\circ = 75.4 \text{ kN}$$

$$P_{a,v} = P_a \sin 10^\circ = 76.6 \sin 10^\circ = 13.3 \text{ kN}$$

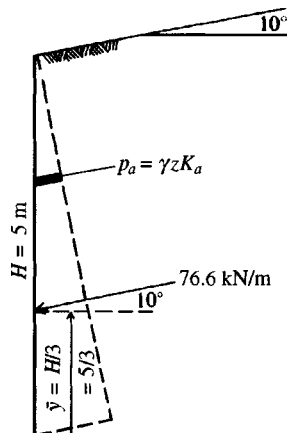


Figure E11-3

////

## 11-6 GENERAL COMMENTS ABOUT BOTH METHODS

One should not use the Rankine method for  $K_p$  when  $\beta > 0$ , since an inspection of Table 11-4 shows that it decreases with increasing  $\beta$ . This is clearly not correct— $K_a$  does properly increase. Note also that one can use a  $(-)$   $\beta$  in the Rankine equations, but the computed coefficients are those of  $(+)$   $\beta$ .



The Coulomb equations are valid for both (+) and (-)  $\beta$ . That is,  $K_p$  increases with increasing  $\beta$  and decreases with (-)  $\beta$  values.

**SOIL WITH COHESION.** Neither the Coulomb nor Rankine method explicitly incorporated cohesion as an equation parameter in lateral earth pressure computations. Bell (1915) seems to be the first person to publish a solution to this problem. Bell's equations are actually Eqs. (2-54) and (2-55) and were directly obtained from Mohr's circle. With these equations for the pressure the wall force is obtained as in Eqs. (11-9) for the cohesionless case by integrating between limits over the depth increment  $dz$ . Modifications to these equations might include using the Coulomb or Rankine  $K$  factors in lieu of the tangent factors.

**Example 11-4.** Draw the active earth pressure diagram for a unit width of wall for the conditions shown in Fig. E11-4a. Compare the several possible alternatives that are produced from this problem (tension crack, how the diagram might be modified, and water in tension crack).

At top:  $z = 0$

$$p_a = \gamma z K_a - 2c \sqrt{K_a} = -2(10.5)(0.84) = -17.64 \text{ kPa}$$

At  $p = 0$ :

$$\gamma z K_a - 2c \sqrt{K_a} = 0 \quad [\text{Set Eq. (2-55)} = 0]$$

and

$$z = \frac{2c \sqrt{K_a}}{\gamma K_a} = \frac{2c}{\gamma \sqrt{K_a}} = \frac{2(10.5)}{17.52(0.84)} = 1.43 \text{ m}$$

*Note:* This value of  $z$  is the depth of a potential tension crack, since (-)  $p$  = tension stresses that the soil cannot carry. At base, the lateral pressure [from Eq. (2-55)] is

$$p_a = 17.52(6.5)(0.704) - 2(10.5)(0.84) = 62.53 \text{ kPa}$$

The resultant force is found as  $\sum F_h = R$ . The location of the resultant may be found by summing moments at the base or by inspection, depending on the complexity of the pressure diagram. The tension zone  $ab$  is usually neglected for finding the magnitude and location of the resultant.

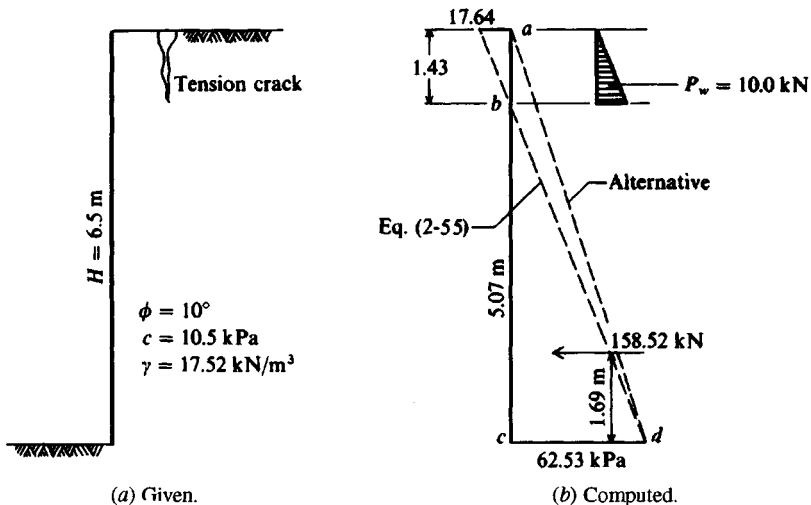


Figure E11-4

**Neglecting the tension zone**

$$R = 62.53 \left( \frac{5.07}{2} \right) = 158.5 \text{ kN/m}$$

$$\bar{y} = \frac{5.07}{2} = 1.69 \text{ m above } c$$

**Using alternative pressure diagram *acd***

$$R = 62.53 \left( \frac{6.5}{2} \right) = 203.2 \text{ kN/m}$$

$$\bar{y} = \frac{6.5}{3} = 2.17 \text{ m (by inspection)}$$

With water in the tension crack,

$$R = 158.5 + \frac{9.807(1.43)^2}{2} = 168.5 \text{ kN/m}$$

and the overturning moment including water in the tension crack is

$$M_o = 158.5(1.69) + 10.0 \left( 5.07 + \frac{1.43}{3} \right) = 323.3 \text{ kN} \cdot \text{m/m}$$

$$\bar{y} = \frac{323.3}{168.5} = 1.92 \text{ m above } c$$

In this case the water-in-crack solution is between the two previous solutions, from which it appears that the alternative pressure diagram *acd* provides a conservative solution.

////

**Example 11-5.** Plot the active earth pressure diagram and compute the resultant  $R$  and its location  $\bar{y}$  for the wall system shown in Fig. E11-5. This type of problem is often encountered in excavations for large structures where there may be two or more basement levels. The soil parameters  $\phi$ ,  $c$  may be estimated or else be obtained from performing consolidated isotropically undrained (CIU) tests on good-quality tube samples. The major approximation is defining the several strata by abrupt discontinuities (using lines as shown to delineate layers). In most real situations the soil type grades through a finite length from one to the next.

**Solution.** We should plot the soil and pressure profiles adjacent to each other as in Fig. E11-5. The Rankine equations for active earth pressure coefficients  $K_a$  will be used [use program FFACTOR since these small  $\phi$  angles are not in Table 11-3, or use Eq. (11-7a)].

For instance, for  $\phi = 32^\circ$ , use Table 11-3, obtain  $K_a = 0.307$  and  $\sqrt{0.307} = 0.554$ , etc.

Typical computations for  $\Delta p'_o$  are as follows:

Depth, m	$\Delta p'_o$ , kPa
0	100 kPa (surcharge)
1.80	$100 + 1.80(17.30) = 131.4 \text{ kPa}$
2.40	$131.4 + 0.6(19.60 - 9.807) = 131.4 + 0.6(9.79)$ $= 137.02 \text{ kPa}$
5.15	$137.02 + 2.75(9.89) = 164.22 \text{ etc.}$

It will be convenient to tabularize the computations as in Table E11-5 following.

Notice that at the interface between two soils we use the interface pressure two times: first with  $-dz$  and the upper  $K$  coefficients, and second with  $+dz$  and the  $K$  coefficients of the lower soil. Note also that the  $2c\sqrt{K_a}$  term can be simplified for the second use.

To find the resultant we must divide the pressure profile into rectangles and triangles as shown on Fig. E11-5b. The water pressure is included ( $K_a = K_p = K_w = 1$ ) if the water cannot drain

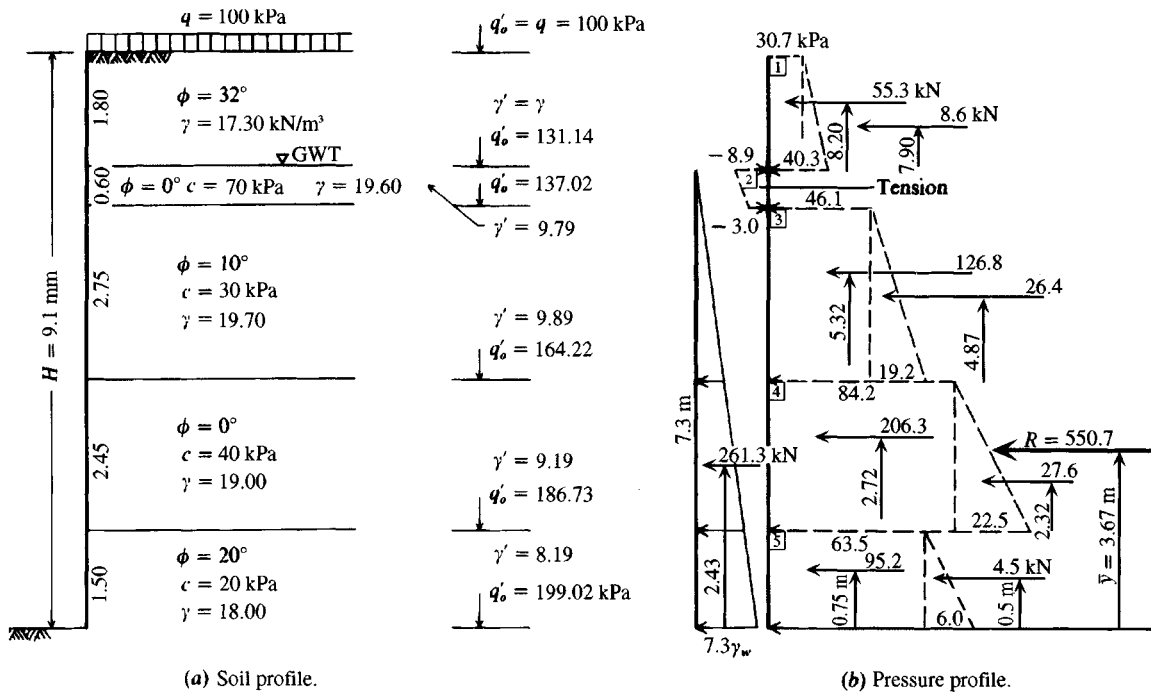


Figure E11-5

TABLE E11-5

Soil	Depth, m	$K_a$	$\sqrt{K_a}$	$\Delta P'_o$ , kPa	Wall pressure, $q_h$ , kPa
1	0	0.307	0.554	100.	$100(0.307) = 30.7$
	$1.80-dz$			131.14	$(131.14)(0.307) = 40.3$
2	$1.80+dz$	1.000	1.000	131.14	$(131.14)(1.00) - 2(70)(1.00) = -8.9$
	$2.40-dz$			137.02	$(137.02)(1.00) - 2(70)(1.00) = -3.0$
3	$2.40+dz$	0.704	0.839	137.02	$(137.02)(0.704) - 2(30)(0.839) = 46.1$
	$5.15-dz$			164.22	$(164.22)(0.704) - 60(0.839) = 65.3$
4	$5.15+dz$	1.000	1.000	164.22	$(164.22)(1.000) - 2(40)(1.00) = 84.2$
	$7.60-dz$			186.73	$(186.73)(1.000) - 80(1.00) = 106.7$
5	$7.60+dz$	0.490	0.700	186.73	$(186.73)(0.490) - 2(20)(0.700) = 63.5$
	9.1			199.02	$(199.02)(0.490) - 40(0.700) = 69.5$

through the wall or away by other means. Since the water contribution is significant, it is obvious that drainage should be allowed if possible.

The tension zone ( $-$ )  $q_h$  is a problem. Should it be included to reduce the wall force or neglected, as it may pull away from the wall? A more conservative case is made if the tension zone is neglected, which we will do here—so *neglect tension zone*.

There is much busywork with this type of problem—particularly to get the pressure profile—so that a computer program such as B-25 should be used if possible.

Computations for finding the resultant are as follows:

1. Compute the force  $P_i$  for each geometric area (rectangle or triangle) and locate its resultant  $\bar{y}$  from the base as partially shown on Fig. E11-5b:

$$P_1 = 30.7(1.80) = 55.3 \text{ kN}$$

$$P_2 = (40.3 - 30.7)1.80/2 = 8.6 \text{ kN}$$

$$P_3 = 46.1(2.75) = 126.8 \text{ kN} \quad \text{etc.}$$

2. Sum the horizontal forces  $\sum F_h = R$

$$R = 55.3 + 8.6 + 126.8 + 26.4 + 206.3 + 27.6 + 95.2 + 4.5 \\ = 550.7 \text{ kN}$$

The water  $P_w = 7.3(9.807)(7.3/2) = 261.3 \text{ kN}$ .

Compute  $y_i$  for each  $P_i$ :

$$y_1 = 1.5 + 2.45 + 2.75 + 0.60 + 1.80/2 = 8.20 \text{ m}$$

$$y_2 = 7.3 + 180/3 = 7.9 \text{ m}$$

$$y_3 = 1.5 + 2.45 + 2.75/2 = 5.32 \text{ m}$$

$$y_4 = 3.95 + 2.75/3 = 4.87 \text{ m} \quad \text{etc.}$$

Compute  $\bar{y}$ :

$$R\bar{y} = \sum_1^n P_i y_i \\ 550.7\bar{y} = 55.3(8.20) + 8.6(7.90) + 126.8(5.32) + 26.4(4.87) \\ + 206.3(2.72) + 27.6(2.32) + 95.2(0.75) + 4.5(0.50) \\ \bar{y} = \frac{2023.36}{550.7} = 3.67 \text{ m} \quad (\text{above base of wall})$$

The soil pressure resultant and corresponding  $\bar{y}$  are shown on Fig. E11-5b (and this calculation does not include water).

////

## 11-7 ACTIVE AND PASSIVE EARTH PRESSURE USING THEORY OF PLASTICITY

The Coulomb and Rankine passive earth pressure methods consistently overestimate the passive pressure developed in field and model tests for  $\phi$  much over  $35^\circ$ . This estimate may or may not be conservative, depending on the need for the passive pressure value. Because of the problem of overestimation, Caquot and Kerisel (1948) produced tables of earth pressure based on nonplane-failure surfaces; later Janbu (1957) and then Shields and Toluany (1973) proposed an approach to the earth pressure problem similar to the method of slices used in slope-stability analyses. Sokolovski (1960) presented a finite-difference solution using a highly mathematical method. All these methods give smaller values for the passive earth pressure coefficient. None of these methods significantly improves on the Coulomb or Rankine active earth pressure coefficients.

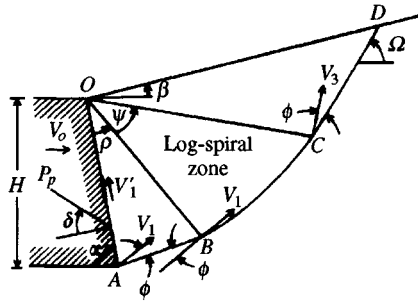
Rosenfarb and Chen (1972) developed a closed-form earth pressure solution using plasticity theory that can be used for both active and passive earth pressure computations. The closed-form solution requires a computer program with an iteration routine, which is not particularly difficult. This method is included here because of the greater clarity over the alternative methods.

Rosenfarb and Chen considered several failure surfaces, and the combination of a so-called *log-sandwich* mechanism gave results that compared most favorably with the Sokolovski solution, which has been accepted as correct by many persons. Figure 11-10 illustrates the passive log-sandwich mechanism. From this mechanism and appropriate consideration of its velocity components the following equations are obtained.

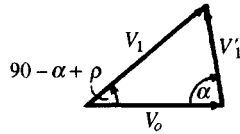
### Cohesionless Soil

For a smooth wall ( $\delta < \phi$ ):

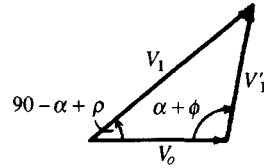
$$\begin{aligned} \left\{ \begin{array}{l} K_{ay} \\ K_{py} \end{array} \right\} &= \frac{\mp \sec \delta}{\mp \sin \alpha + \tan \delta \cos \alpha - [\tan \delta \cos(\alpha - \rho)/\cos \rho]} \\ &\times \left( \frac{\tan \rho \cos(\rho \pm \phi) \cos(\alpha - \rho)}{\sin \alpha \cos \phi} + \frac{\cos^2(\rho \pm \phi)}{\cos \rho \sin \alpha \cos^2 \phi (1 + 9 \tan^2 \phi)} \right) \\ &\times \left\{ \cos(\alpha - \rho) [\pm 3 \tan \phi + (\mp 3 \tan \phi \cos \psi + \sin \psi) \right. \\ &\times \exp(\mp 3 \psi \tan \phi)] \\ &\left. + \sin(\alpha - \rho) [1 + (\mp 3 \tan \phi \sin \psi - \cos \psi) \times \exp(\mp 3 \psi \tan \phi)] \right\} \\ &+ \frac{\cos^2(\rho \pm \phi) \sin(\alpha - \rho - \psi + \beta) \cos(\alpha - \rho - \psi) \exp(\mp 3 \psi \tan \phi)}{\cos \phi \sin \alpha \cos(\alpha - \rho - \psi \mp \phi + \beta) \cos \rho} \end{aligned} \quad (11-10)$$



(a) Passive log-sandwich mechanism with  $V_3 = V_1 \exp(\psi \tan \phi)$ .



(b) Velocity diagram for a smooth wall  $\delta < \phi$ .



(c) Velocity diagram for a rough wall  $\delta = \phi$ .

**Figure 11-10** Plastic stress fields for earth pressure using the theory of plasticity. [Rosenfarb and Chen (1972).]

For a rough wall ( $\delta = \phi$ ):

$$\begin{aligned}
 \left\{ \begin{array}{l} K_{ay} \\ K_{py} \end{array} \right\} &= \frac{\mp \sec \delta}{\mp \sin \alpha + \tan \delta \cos \alpha} \left( \frac{\sin^2 \rho \cos(\rho \pm \phi) \cos(\alpha - \rho) \sin(\alpha \mp \phi)}{\sin^2 \alpha \cos \phi \cos(\rho \mp \phi)} \right. \\
 &\quad \mp \frac{\cos^2(\rho \pm \phi) \sin(\alpha \mp \phi)}{\sin^2 \alpha \cos^2 \phi (1 + 9 \tan^2 \phi) \cos(\rho \mp \phi)} \\
 &\quad \times \left\{ \cos(\alpha - \rho) [\pm 3 \tan \phi + (\mp 3 \tan \phi \cos \psi + \sin \psi) \exp(\mp 3 \psi \tan \phi)] \right. \\
 &\quad \left. + \sin(\alpha - \rho) [1 + (\mp 3 \tan \phi \sin \psi - \cos \psi) \exp(\mp 3 \psi \tan \phi)] \right\} \\
 &\quad + \frac{\cos^2(\rho \pm \phi) \sin(\alpha - \rho - \psi + \beta) \cos(\alpha - \rho - \psi) \sin(\alpha \mp \phi) \exp(\mp 3 \psi \tan \phi)}{\sin^2 \alpha \cos \phi \cos(\alpha - \rho - \psi + \beta \mp \phi) \cos(\rho \mp \phi)} \Bigg) \\
 &\quad (11-11)
 \end{aligned}$$

## Cohesive Soil

For a smooth wall ( $\delta < \phi$ ):

$$\begin{aligned}
 \left\{ \begin{array}{l} K_{ac} \\ K_{pc} \end{array} \right\} &= \frac{\sec \delta}{\mp \sin \alpha + \tan \delta \cos \alpha - [\tan \delta \cos(\alpha - \rho) / \cos \rho]} \\
 &\quad \times \left\{ \tan \rho + \frac{\cos(\rho \pm \phi) \sin(\alpha - \rho - \psi + \beta) \exp(\mp \psi \tan \phi)}{\cos \rho \cos(\alpha - \rho - \psi \mp \phi + \beta)} \right. \\
 &\quad \left. \mp \frac{\cos(\rho \pm \phi) [\exp(\mp 2 \psi \tan \phi) - 1]}{\sin \phi \cos \rho} \right\} \\
 &\quad (11-12)
 \end{aligned}$$

For a rough wall ( $\delta = \phi$ ):

$$\left\{ \begin{array}{l} K_{ac} \\ K_{pc} \end{array} \right\} = \frac{\sec \delta}{\mp \sin \alpha + \tan \delta \cos \alpha} \left\{ \begin{array}{l} \frac{\cos \phi \cos(\alpha - \rho)}{\sin \alpha \cos(\rho \mp \phi)} + \frac{\sin \rho \sin(\alpha \mp \phi)}{\sin \alpha \cos(\rho \mp \phi)} \\ + \frac{\cos(\rho \pm \phi) \sin(\alpha - \rho - \psi + \beta) \sin(\alpha \mp \phi) \exp(\mp \psi \tan \phi)}{\sin \alpha \cos(\alpha - \rho - \psi \mp \phi + \beta) \cos(\rho \mp \phi)} \\ \mp \frac{\cos(\rho \pm \phi) \sin(\alpha \mp \phi) [\exp(\mp 2\psi \tan \phi) - 1]}{\sin \phi \sin \alpha \cos(\rho \mp \phi)} \end{array} \right\} \quad (11-13)$$

In solving Eqs. (11-10) through (11-13), it is necessary to solve for the maximum value of  $K_p$  or  $K_a$ . The maximizing of these equations depends on the two variables  $\rho$  and  $\psi$ . This requires a search routine in computer program B-23. The values of the two dependent variables are initialized to approximately

$$\rho \cong 0.5(\alpha + \beta)$$

$$\psi \cong 0.2(\alpha + \beta)$$

With these initial values, the search routine is used to revise the values until convergence is obtained. In most cases values from which  $K_p$  is computed are found after not more than 20 iterations. A computer program should shut off after 46 to 50 iterations. In a few cases the program may not find a solution using the above initial values because of the programming search routine. For these cases, one must change the initial values and retry as necessary to obtain the solution. Table 11-5 gives selected values of  $K_p$  for cohesionless soils. Note that these equations correctly give  $K_p$  increasing with  $\beta$ . Values of  $\beta = \delta = 0$  are not shown, as they are identical to the Coulomb or Rankine solution.

The "smooth" wall solution is used for wall friction  $\delta < \phi$ ; when  $\delta = \phi$  the "rough" wall equation is used. Equations (11-12) and (11-13) can readily be programmed, using the same routines to solve an equation for minimum or maximum with two dependent variables, to obtain passive pressure coefficients for cohesive soil. This solution does not give greatly different values from the Coulomb passive pressure theory until the  $\phi$  angle becomes larger than  $35^\circ$  and with  $\delta$  on the order of  $\phi/2$  or more and  $\beta \neq 0^\circ$  (since the back slope can have  $\pm \beta$ ).

## 11-8 EARTH PRESSURE ON WALLS, SOIL-TENSION EFFECTS, RUPTURE ZONE

The Rankine or Coulomb earth pressure equations can be used to obtain the force and its approximate point of application acting on the wall for design. Soil-tension concepts can also be investigated. These will be taken up in the following discussion.

### 11-8.1 Earth Forces on Walls

From Eq. (2-55) and temporarily considering a soil with  $c = 0$ ,  $\gamma$  constant with depth  $z$  and referring to Fig. 11-9a, we can compute the wall force as

$$P_a = \int_0^H \sigma_3 K_a dz = \int_0^H \gamma z K_a dz = \frac{\gamma z^2 K_a}{2} \bigg|_0^H = \frac{\gamma H^2}{2} K_a \quad (a)$$

from which it is evident that the soil pressure diagram is hydrostatic (linearly increases with depth) as shown in the figure. If there is a surcharge  $q$  on the backfill as shown in Fig. 11-9c (other surcharges will be considered in Sec. 11-13), the wall force can be computed as

TABLE 11-5

Selected values of  $K_p$  using limit analysis for  $\alpha = 90^\circ$  (vertical wall) for a granular soil. Values same as in Table 11-2 for  $\beta = 0^\circ$ . Intermediate values may be obtained by plotting  $K_p$

$\beta$	$\phi = 30^\circ$	$35^\circ$	$40^\circ$	$45^\circ$
$\delta = 0$				
-10	2.21	2.65	2.68	3.90
10	4.01	5.20	6.68	8.93
20	5.25	7.03	9.68	13.8
30	6.74	9.50	14.0	21.5
$\delta = 10$				
-10	2.77	3.44	4.3	5.5
10	5.70	7.61	10.4	14.9
20	7.79	10.9	15.9	24.4
30	10.3	14.7	23.6	39.6
$\delta = 20$				
-10	3.56	4.61	6.1	8.2
10	7.94	11.2	16.3	24.9
20	11.2	16.5	25.6	42.4
30	15.1	23.2	41.0	70.2
$\delta = 30$				
-10	4.5	6.2	8.6	12.4
10	10.6	15.8	24.6	40.7
20	15.2	23.2	39.5	70.3
30	20.8	34.8	62.0	0*

\*No solution after 46 iterations.

$$P_a = \int_0^H (\gamma z + q) K_a dz = \left( \frac{\gamma H^2}{2} + qH \right) K_a \quad (b)$$

The point of application requires taking moments about a convenient point, and for the case with surcharge and from the top of the wall we have

$$P_a y = \int_0^H (\gamma z + q) K_a z dz = \left( \frac{\gamma H^3}{3} + \frac{qH^2}{2} \right) K_a \quad (c)$$

and, inserting the value of  $P_a$  from Eq. (b), the distance from the top of the wall is

$$\bar{y}_t = \frac{1}{3} \frac{2\gamma H^2 + 3qH}{\gamma H + 2q}$$

and from the bottom of the wall  $\bar{y} = H - \bar{y}_t$

$$\bar{y} = \frac{H}{3} \frac{3q + \gamma H}{2q + \gamma H} \quad (\text{for } c = 0) \quad (11-14)$$



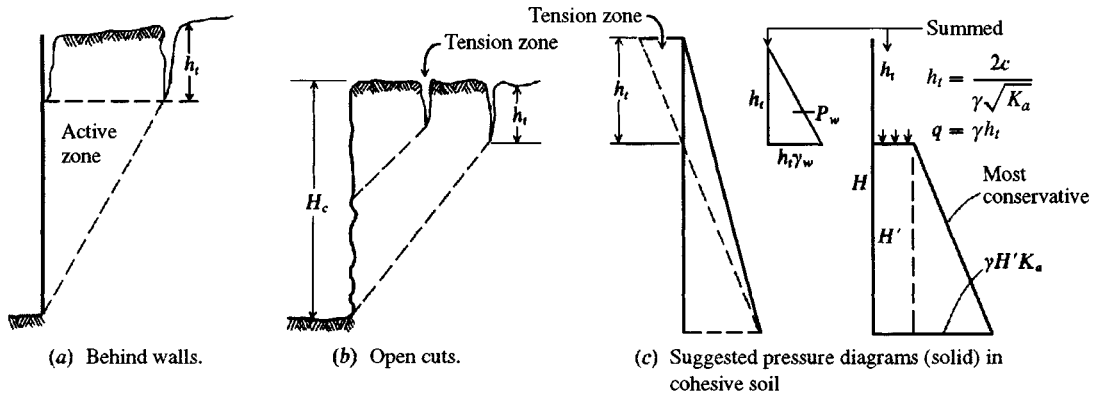


**Figure 11-11** Tension crack and critical depth of an unbraced excavation. Tension cracks are often readily visible adjacent to excavations.

When the surcharge  $q = 0$ , we obtain  $\bar{y} = H/3$ ; for  $c > 0$  locate  $\bar{y}$  using Example 11-4 or Fig. 11-11c as a guide. It is not correct to convert the surcharge to an equivalent additional wall height and use  $\bar{y}$  to the centroid of a triangle, because the surcharge effect is rectangular against the wall.

A number of researchers using both models and fairly large retaining walls have found that the wall force resultant seldom acts at the distance  $\bar{y} = H/3$  from the wall base. This implies that the wall pressure diagram is not triangular. Williams (1989, with a number of references) derived equations that tend to produce a somewhat parabolic pressure distribution, which may or may not coincide with the Coulomb pressure profile near the top.

In any case, the resultant of the lateral pressure is commonly taken as  $H/3$  and the pressure diagram is assumed to be triangular (if there is no surcharge), including cases where the backfill slope angle  $\beta \neq 0$ . Some evidence exists that, because the wall rotates about its base, the pressure diagram is not triangular and that the resultant is somewhere in the middle one-third of the wall height—about the  $0.4H$  point above the base.

Most walls are constructed with a void on the backfill side, which is then stage-filled and compacted (that is, add a layer, compact it, add another layer, compact it, etc.) until the surface is reached. This method also tends to increase the wall pressure—particularly near the bottom—and more particularly for clay backfills (which may be necessary if granular backfill is not available). The lower compacted soil produces lateral displacements in the upper wall zone, so soil later compacted in this area may not produce enough additional deflection to reduce the lower wall pressure to an active state.

Clayton et al. (1991) measured compaction pressures against a wall from a clay backfill. They found that compaction pressures did not become significant until the air-void content (difference between the zero-air-voids curve and the maximum dry density) was less than 15 percent and that the pressures could be expressed as a percentage of  $s_u$ , ranging from about 20 to 40 percent. Also they found that the lateral pressure, partially produced by compaction, tended to reduce with time. The question is, what to do?

**CHOOSE A  $K$  VALUE.** Overdesign the wall by using a  $K$  intermediate between  $K_a$  and  $K_o$ .

**MAKE ASSUMPTIONS.** Assume the computed soil pressure resultant is above the usual point of application (the one-third point for no surcharge). If the pressure resultant (no

surcharge) is assumed to be at a point above the one-third point, the only way this can be achieved is to force a trapezoidal pressure diagram into the model. This can substantially increase the bending moments for structural walls, but the shear (and soil pressure resultant  $R$ ) remains the same, unless  $R$  is increased by some uncertainty factor, such as 1.1, 1.4, 1.5, and so forth.

We can derive a general equation for locating the pressure resultant and the pressure at the top of the wall necessary to define a trapezoidal pressure diagram. We already know that the bottom pressure  $q_b = \gamma_s H$ . From a trapezoid pressure diagram with  $q_t$  and  $q_b$  and height  $H$  and the pressure resultant located at  $kH$  we can obtain two equations. The resultant  $R = \text{area of a trapezoid}$ , giving

$$R = Hq_t + (q_b - q_t)\frac{H}{2} \rightarrow q_t + q_b = \frac{2R}{H} \quad (a)$$

Use Eq. (9-2) (the location of the center of a trapezoid) as the second equation and substituting  $q_t$  and  $q_b$  for  $a$  and  $b$ , obtain

$$\bar{y} = \frac{H}{3} \left( \frac{2q_t + q_b}{q_t + q_b} \right) = kH \quad (b)$$

Now substitute Eq. (a) into Eq. (b) and simplify to obtain

$$\left. \begin{aligned} q_t &= \frac{2R}{H}(3k - 1) \\ q_b &= \frac{2R}{H}(2 - 3k) \end{aligned} \right\} \quad \text{valid from } \frac{1}{3} \leq k < \frac{2}{3} \quad (11-15)$$

For  $q_{b,\text{init}} = 40$  kPa,  $H = 10$ , compute  $R = 40 \times 10/2 = 200$ . For  $k = \frac{1}{3}$  we have  $q_t = 0$ ;  $q_b = q_{b,\text{init}} = 40$ . For  $k = 0.5$  we have  $q_t = q_b = 20$  {and the new  $R = [(20 + 20)/2](10) = 200$  as before} but now  $\bar{y} = 5$  instead of  $\frac{10}{3}$ . Before computing the new top and base pressures we may increase (or decrease)  $R$  as deemed necessary for the given wall.

One should adjust  $R$  with care—probably it is best to increase the earth pressure coefficient—since available evidence indicates the initial resultant  $R_{\text{init}}$  is about that from the Coulomb/Rankine equation but the location is not. Make the reduction as follows.

Although it is not unreasonable to put the location of the resultant above the one-third point, one must decide what the minimum pressure will be that the wall must resist before failure. A high pressure above the minimum active value may reduce to the minimum active value as the wall starts to rotate forward under the higher pressure. This movement decreases the pressure, but the wall may rotate further still under the reduced lateral pressure. The wall either breaks or shears off or reaches some equilibrium resisting lateral pressure, and movement stops.

## 11-8.2 Soil-Tension Effects on Backfill and Open Trenches

Visible tension cracks usually develop where

1. Cohesive soil is used for backfill.
2. A trench or basement excavation is made in cohesive soil.

In the excavation case the cracks form parallel to the excavation and if under pavements and structures can produce damage. We may use Eq. (2-55), slightly modified and repeated here as

$$\sigma_3 = (q + \gamma z)K_a - 2c\sqrt{K_a} \quad (c)$$

where the quantity  $(q + \gamma z) = \sigma_1$ . Tension exists in a cohesive soil to some depth  $z = h_t$  until the stress  $\sigma_3 = 0$  (after that the stress is compression). This depth is estimated from Eq. (c) by rearranging, replacing  $z$  with  $h_t$ , and solving to obtain

$$h_t = \frac{2c\sqrt{K_a} - qK_a}{\gamma K_a} \quad (11-16)$$

Note the inclusion of the surcharge  $q$  makes this equation general. The equation is most often seen without the surcharge term as follows:

$$h_t = \frac{2c}{\gamma\sqrt{K_a}} \quad (11-16a)$$

The tension crack can form at the wall-soil interface and/or at some distance back from the wall (see Figs. 11-11a, b). It is not unusual for several approximately parallel tension cracks to form.

Another value of interest is the theoretical depth an excavation can stand without lateral bracing. The key words here are the *theoretical depth*. Building codes and governmental safety divisions (OSHA in the United States) usually give limitations on unbraced excavation depths. In any case the theoretical value is computed by integrating Eq. (d) and using  $z = H_c$  = theoretical or critical depth to obtain:

$$P = \int_0^{H_c} \left[ (q + \gamma z)K_a - 2c\sqrt{K_a} \right] dz$$

Integrating (constant = 0), inserting the limits, setting the horizontal force  $P = 0$ , and simplifying, we obtain

$$H_c = \frac{4c}{\gamma\sqrt{K_a}} - \frac{2q}{\gamma} \quad (11-17)$$

There may be some question of what to use for  $K_a$  in Eqs. (11-16) and (11-17) when  $\beta > 0$ , since Eq. (2-55) as developed was for a horizontal ground surface. In the absence of any better information use the Coulomb values from Table 11-3 with  $\delta = 0$ .

One should not rely on the tension zone (see Fig. 11-11c) to reduce lateral pressures. Instead one should assume that it can form and will possibly fill with water.<sup>1</sup> The depth of water (not the quantity) can increase the overturning pressure against the wall considerably owing to both the hydrostatic force of  $\gamma_w h_t$  and the larger moment arm caused by combining the hydrostatic force with the already existing lateral pressure.

<sup>1</sup>If the crack fills with water it will usually close with time as the soil swells. The soil-excavation system must, however, survive during this time, so it is conservative to consider a crack filled with water as a worst case.

It is suggested that when there is a wall tension zone you use either of the two alternatives of Fig. 11-11c, together with the water pressure profile shown, if the tension crack can fill with water. Treating the tension block as a surcharge is probably more nearly correct and gives a more conservative (larger) wall force and overturning moment.

One cannot rely on Eq. (11-17) to predict the critical embankment height accurately for several reasons:

1. Once the tension crack forms, Eq. (2-55) is not valid for the full depth of the excavation.
2. Cohesive soils tend to lose cohesion when exposed in excavations as a result of moisture adsorption and/or shrinkage cracks.
3. A surcharge effect results from equipment and materials piled on the ground adjacent to the excavation.

Because of these several factors, Eq. (11-17) should include a safety factor for design to obtain a design depth  $H'_c$ , as

$$H'_c = \frac{1}{\text{SF}} \left[ \frac{4c}{\gamma \sqrt{K_a}} - \frac{2q}{\gamma} \right] \quad (11-17a)$$

Of course, if local authorities require a lesser value of  $H'_c$ , that should be used.

### 11-8.3 Rupture Zone

The solution of the Rankine equations as shown by the Mohr's circle of Fig. 11-1a gives the rupture slope  $\rho$  in the backfill as

$$\rho = 45 \pm \frac{\phi}{2} \quad (+) = \text{active pressure case}$$

for horizontal ( $\beta = 0$ ) ground. For the general case of sloping ground and/or wall friction the  $\rho$  angle is not that given above. For these cases it is recommended to use the trial wedge computer program B-7 on your diskette to obtain the critical  $\rho$  angle (so as to locate the potential slip zone) since it is given as part of the output for hand checking. There are closed-form solutions as in Jumikis (1962); however, they are complicated and subject to error in either derivation or typesetting so that they should be used very cautiously if at all.

## 11-9 RELIABILITY OF LATERAL EARTH PRESSURES

Several sets of wall tests have been performed to check the validity of the Coulomb and Rankine active and passive earth pressure methods. These include the tests of Terzaghi (1934), Peck and Ireland (1961), Rowe and Peaker (1965), Mackey and Kirk (1967), James and Bransby (1970), Rehnman and Broms (1972), and Coyle et al. (1972). Field and model tests [as by Fang and Ishibashi (1986)] tend to confirm the active earth pressure concept reasonably well if the backfill is carefully placed so that compaction effects do not create excessive stresses and if the wall rotates and/or translates sufficiently to mobilize the maximum shearing resistance in the soil. Often the top of the wall translates/rotates adequately while near the stem base it does not so that the pressure near the base is larger than predicted by theory—particularly if some compaction of the backfill has been done. Regardless, the total wall force from numerically integrating the pressure profile is usually close to the theoretical “active”

value and the resultant is usually at or above the lower one-third point (often closer to 0.4 or  $0.45H$ ).

The active zone rupture surface is also fairly close to that predicted by theory and close to being a plane. The passive zone, however, often is not in close agreement and the rupture surface is closer to being a spiral. This latter gives additional cause for suggesting the use of Sec. 11-7 with computer program B-23 (or similar) for the passive earth pressure case.

## 11-10 SOIL PROPERTIES FOR LATERAL EARTH PRESSURE COMPUTATIONS

It is evident from the use of the Mohr's circle as a starting point for earth pressure coefficients that *effective* stresses together with any hydrostatic water pressure are used to compute the wall force. The usual condition of soil behind walls is as shown in Fig. 11-12. We have excavated a vertical or sloping space for the wall, poured the wall footing and wall and then backfilled the zone previously excavated, usually with some compaction. We then have to idealize the model somewhat to compute the earth force that the wall must resist.

### 11-10.1 Soil Parameters

These soil parameters are used in computing lateral earth pressure:

1. Drained values for sand are used for reasons cited in Chap. 2. Ideally, plane strain  $\phi$  values as obtained from direct shear, direct simple shear, or from triaxial values that have

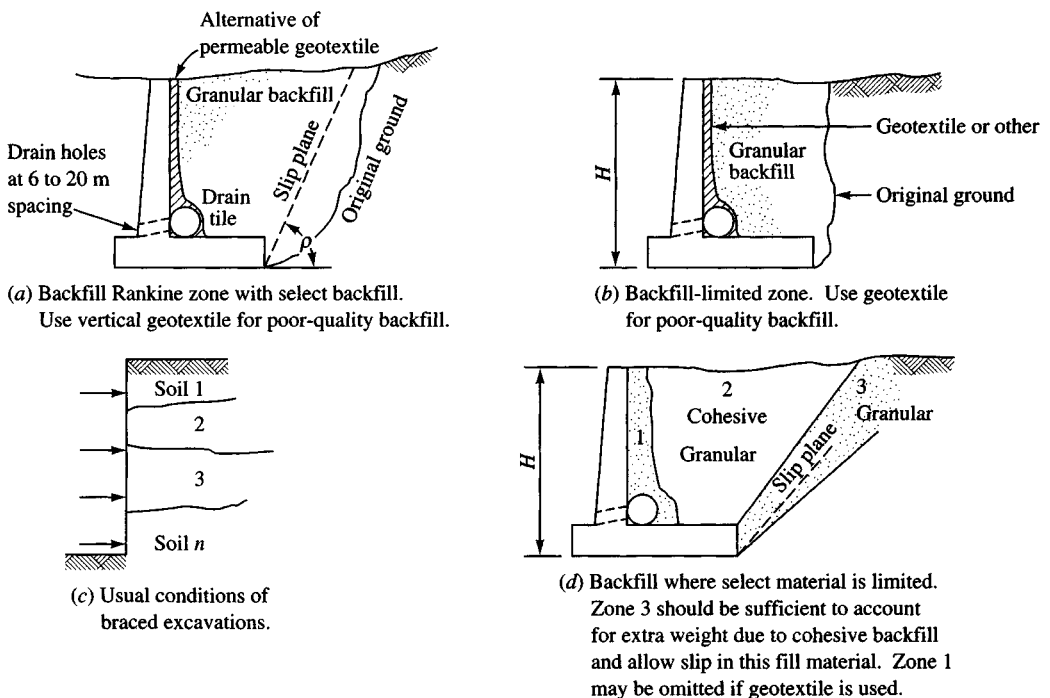


**Figure 11-12** Various backfill conditions. The longitudinal collector (or drain) pipe is optional.

been adjusted to plane strain values are employed. However, very commonly a  $\phi$  value is estimated from visual examination of the sand and using a conservative value from 30 to 34°.

2. For cohesive soils  $s_u$  values are commonly used and are generally adequate for normally and lightly overconsolidated soil.
3. For overconsolidated soil we may use these:
  - a. A drained strength parameter with  $\phi'$  obtained from a drained shear test, using Fig. 2-25 as a test guide (not often), or estimated from one of the correlations given on Figs. 2-35 or 2-36.
  - b. The undrained shear strength at the creep threshold.
  - c. A drained  $\phi$  angle between peak and residual strength.

In cohesive soil a wall designed using almost any set of reasonable design strength parameters is likely to have an adequate risk factor if the following conditions are met:

1. Wall excavation did not cave during wall construction.
2. Excavated zone is backfilled and compacted using a freely draining soil.
3. If backfill is cohesive, increase the  $k$ -factor of Eq. (11-15) to 0.40 to 0.50.

The risk factor is likely adequate even if the excavation/backfill zone is fairly limited since a cave-in would have occurred if the retained soil were inherently unstable.

## 11-10.2 Water in Backfill

Water in the backfill soil is particularly undesirable since it increases the unit weight and lateral pressure. If a water table can form (or stabilize), the effect is considerably worse since the  $\phi$  angle of water is zero, giving  $K_a = K_p = 1$  as used earlier. A further undesirable side effect in cold climates is that the backfill water may freeze and greatly increase the lateral pressure, causing the wall to displace forward. This displacement is usually not fully recovered when thawing occurs.

Most of the water problem can be avoided by constructing drain (or weep) holes through the wall base or using lateral drain pipes. The major problem here is to ensure that the backfill does not erode through the weep holes or clog the lateral drain pipes. If sand is used it should be properly graded, with coarse material adjacent to the drainage device and finer material over the coarse. Currently a more reliable method is to face the backfill side of the wall with a geotextile especially fabricated to allow vertical drainage. The backfill adjacent to the geotextile does not have to be carefully graded for the geotextile prevents soil erosion. It can be placed vertically and draped over the lateral drains to avoid clogging. This material will allow the use of either granular (always preferable) or cohesive backfill.

Although a geotextile material is ideal for allowing backfill drainage it is initially more costly and requires care in placing and backfilling. Offsetting the higher initial cost is the savings accrued from reduced maintenance, i.e., regular inspections and recovering eroded material (refer to Fig 12-18b) from the weep hole exits and putting it back behind the wall (often in vertical "pipes" formed by erosion down to the weep holes).

### 11-10.3 Angle of Wall Friction $\delta$

Wall friction apparently depends not only on the soil properties but also on the amount and direction of wall movement [see Sherif et al. (1982)]. Indications are that maximum wall friction may not occur simultaneously with maximum shearing resistance along the rupture surface and that wall friction is not a constant along the wall—probably because the relative soil-wall movement is not constant.

Considerable engineering judgment must be applied to obtain realistic values of wall friction since they are pressure-dependent. Values of  $\delta = 0.6$  to  $0.8\phi$  are reasonable for concrete walls where forms are used giving a relatively smooth backface. Table 11-6 gives several values of  $\delta$  for other wall-to-soil materials. For steel, concrete, and wood the values shown are for a normal pressure  $\sigma_n$  of about 100 kPa. Decrease the values about 2 degrees for each 100 kPa increase in sand [see Acar et al. (1982) and Fig. 2-31].

Rankine earth pressure is commonly used for the structural design of low- and medium-height walls, since a larger wall pressure is obtained from not including any wall friction angle  $\delta$ . For high walls (say more than about 6 m) one should consider using the Coulomb

**TABLE 11-6**  
**Friction angles  $\delta$  between various foundation materials and soil or rock\***

Interface materials	Friction angle, $\delta$ , degrees†
Mass concrete or masonry on the following:	
Clean sound rock	35°
Clean gravel, gravel-sand mixtures, coarse sand	$\phi$
Clean fine to medium sand, silty medium to coarse sand, silty or clayey gravel	$\phi$
Clean fine sand, silty or clayey fine to medium sand	$\phi$
Fine sandy silt, nonplastic silt	$\phi$
Very stiff and hard residual or preconsolidated clay	$\phi$
Medium stiff and stiff clay and silty clay	$\phi$
Steel sheet piles against the following:	
Clean gravel, gravel-sand mixture, well-graded rock fill with spalls	22°
Clean sand, silty sand-gravel mixture, single-size hard rock fill	17
Silty sand, gravel, or sand mixed with silt or clay	14
Fine sandy silt, nonplastic silt	11
Formed concrete or concrete sheetpiling against the following:	
Clean gravel, gravel-sand mixtures, well-graded rock fill with spalls	22–26
Clean sand, silty sand-gravel mixture, single-size hard rock fill	17–22
Silty sand, gravel, or sand mixed with silt or clay	17
Fine sandy silt, nonplastic silt	14
Various structural materials	
Masonry on masonry, igneous and metamorphic rocks:	
Dressed soft rock on dressed soft rock	35°
Dressed hard rock on dressed soft rock	33
Dressed hard rock on dressed hard rock	29
Masonry on wood (cross grain)	26
Steel on steel at sheet-pile interlocks	17
Wood on soil	14–16‡

\*May be stress-dependent (see text) for sand.

†Single values  $\pm 2^\circ$ . Alternate for concrete poured on soil is  $\delta = \phi$ .

‡May be higher in dense sand or if sand penetrates wood.

earth pressure (with some estimated wall friction angle  $\delta$ ), as the Rankine pressure is likely to produce too much wall overdesign.

#### 11-10.4 Wall Adhesion

Wall adhesion develops from any cohesion in the soil. In the upper region it is expected a tension crack may form (or form during dry periods as the ground naturally shrinks). The value of adhesion  $c_a$  below the tension crack is usually taken at from 0.5 to  $0.7s_u$  with a maximum value not much over 50 kPa. There is some opinion to neglect the tension zones along a wall (see Examples 11-4 and 11-5). One may need to investigate both the total stress case [with cohesion ( $s_u$ )] and the drained (effective) stress case using only  $\phi'$ , depending on the particular problem parameters.

### 11-11 EARTH-PRESSURE THEORIES IN RETAINING WALL PROBLEMS

Both the Rankine and Coulomb methods are widely used to compute the lateral earth pressure on retaining walls. The Rankine solution is often used because the equations are simple and are somewhat more conservative than the Coulomb equations, that is, they compute a larger lateral pressure.

The Rankine (and Coulomb) equation for cohesionless soil and no surcharge has the same form as for hydrostatic problems, that is,

$$P_a = \frac{H}{2}\sigma_h = \frac{H}{2}(\gamma HK_a)$$

where the  $\gamma K_a$  term is the equivalent unit weight of some fluid. Values in the range of 5 to 8 kN/m<sup>3</sup> are given in some handbooks, and when these values are used, the resulting design is termed the *equivalent fluid method*. This procedure is not generally recommended, partly because one can simply select some value and not really analyze the problem.

In using either the Rankine or Coulomb solutions, no part of the wall should interfere with the formation of the approximate rupture surface (line  $BC$  of Fig. 11-2). Generally for cantilever retaining walls (walls with a heel projection as in Fig. 11-13b) one must make two solutions:

1. At the back face of the wall using  $H = AB$  of Fig. 11-13b so the stem can be designed to resist shear and moment.
2. At the heel point  $C$  using  $H = A'C$  for overall wall sliding and overturning stability.

#### 11-11.1 Walls with Limited Backfill Zones

A major consideration in wall design is whether the idealized rupture zone can form as illustrated in Fig. 11-12. In Fig. 11-12a the backfill zone is large enough that the “Rankine” zone can develop in soil of known properties. In Fig. 11-12b the backfill zone is limited and the Rankine zone (if one develops) will be in the original ground—the granular backfill only provides free drainage so hydrostatic water pressure does not form. Obviously, if the existing ground has been standing for some time it will contribute little—if any—lateral pressure to the wall and the principal wall pressure will be from compacting the backfill in the limited zone; however, lateral pressure from compaction may be substantial and even exceed any computed active pressure.



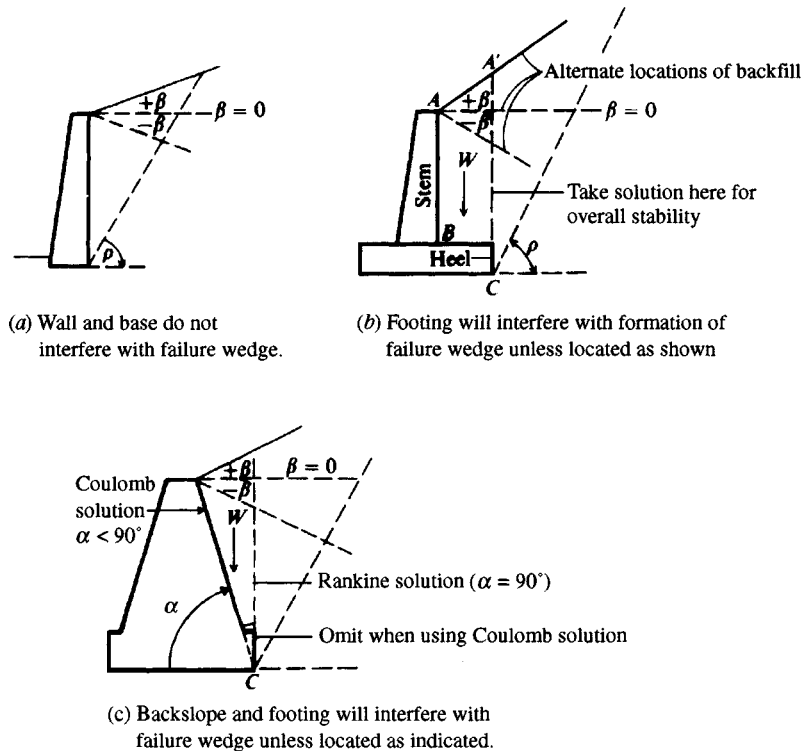


**Figure 11-13** Rankine wedge locations for valid solutions. In (b) and (c) include weight  $W$  in stability computations.

The actual wall pressure in this case depends on wall rigidity (in terms of displacement) and compaction effort. Usually compaction-induced wall pressures produce a resultant wall force close to midheight versus the one-third height for the active pressure case. This problem was discussed in Sec. 11-8.1, where it was given that one may use a lateral earth pressure coefficient

$$K_a \leq K \leq K_o$$

and either locate the resultant at the one-third point or use Eq. (11-15) to locate the resultant higher along the wall.

Figure 11-12b represents a common field situation where considerable engineering judgment is required to estimate the wall pressures. Considerable opinion holds that, when the  $b$  dimension shown on the figure is so narrow that the Rankine wedge does not form, some kind of arching action occurs. Handy (1985) considered arching in some detail and later Frydman and Keissar (1987) suggested that one might estimate the lateral pressure using a modification of Eq. (11-24) of Sec. 11-16 to read

$$\sigma_h = \frac{\gamma b}{2 \tan \delta} \left[ 1 - \exp(-2K \frac{z}{b} \tan \delta) \right] \quad (11-18)$$

where  $\gamma$  = unit weight of backfill  
 $b$  = backfill zone width

$\tan \delta$  = coefficient of friction

$z$  = depth from top to where the lateral pressure  $\sigma_h$  is computed

$K$  = lateral pressure coefficient

The value of  $K$  is critical—some use  $K = K_a$ , others use  $K = K_o$ , and still others use some intermediate value. It would appear reasonable to use  $K_a$  if the wall can rotate and  $K_o$  if the wall is rigid. Frydman and Keissar (1987) also give an equation for estimating  $K$  that depends on  $\phi$  and  $\delta$  as follows:

$$K = \frac{(\sin^2 \phi + 1) - \sqrt{(\sin^2 \phi + 1)^2 - (1 - \sin^2 \phi)(4 \tan^2 \delta - \sin^2 \phi + 1)}}{(4 \tan^2 \delta - \sin^2 \phi + 1)} \quad (11-19)$$

For  $\phi = 32^\circ$  and  $\delta = 18^\circ$  one obtains  $K = 0.329$ . The Rankine  $K_a = 0.307$  but it has no provision for including the wall friction angle  $\delta$ . This equation is somewhat sensitive to  $\delta$ , so one should exercise care to try to estimate a “best” value. Equation (11-19) is programmed into program FFACTOR as option 8 on your program diskette.

Figure 11-12d presents a method where granular backfill is limited in availability, so some is placed to locate the “Rankine” zone adequately and then poor material is used in the region where it is not critical. The limited back face zone is for drainage and could be eliminated by using a vertical drainage geotextile against the wall. Here one would use the  $\phi$  angle of the granular soil but a unit weight that is an average for the backfill. Since this backfill geometry requires careful field control, its use is a last resort.

### 11-11.2 Sloping and Irregular Backfill Surface

When the backfill is smooth or even, it may either be horizontal or have a  $\pm\beta$  angle as illustrated in Fig. 11-13. The Rankine equations see only a (+)  $\beta$  angle, but the Coulomb equations recognize the  $\beta$  angle and its sign.

Additionally we may have a sloping dredge line (of Fig. 11-2). We would intuitively expect a (+) slope to increase the wall pressure and a (–) to decrease the pressure. This expectation is reflected in the Coulomb and Theory of Elasticity methods for both (+) and (–)  $\beta$  values and in the Rankine method for (+) values. The (–) values have particular value for walls using passive pressure in the soil below the dredge line. Occasionally walls supporting coal piles and the like may have a negative slope as the stored material is depleted.

Where the ground is irregular, we may estimate the exit of the Rankine zone (line AC of Fig. 11-7) and in region BC treat the irregular surface as either a best-fit slope or as a uniform surcharge and use the equations for the case; for example in Fig. 11-14a we might smooth out the irregular slope B'FE, measure the resulting  $\beta$  angle, and use either the Rankine or Coulomb equation to obtain a lateral pressure coefficient.

Alternatively, we may also use the trial wedge method in Sec. 11-11.3, particularly if we want a better estimate of the location of the rupture line.

### 11-11.3 Surcharges on Backfill

Surcharges such as point, line, strip, or finite area loads may be on the backfill and increase the lateral pressure. Neither the Coulomb nor the Rankine equations have provision for these types of surcharges. The graphical and computer methods of the next section and the Theory of Elasticity method of Sec. 11-13 are often used to obtain lateral earth pressures for backfill loads.

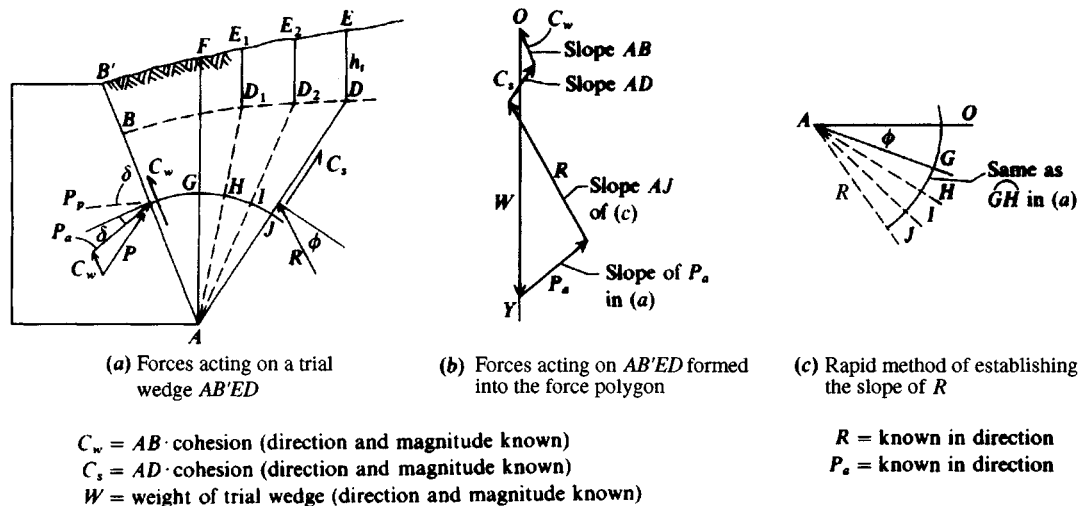


**Figure 11-14** The trial wedge active force solution. For passive force slope of  $P_p$  is shown; slope  $R$  changes,  $C_s$ ,  $C_w$  reverse directions.

From the several solutions by these methods shown in Table 11-7 (Sec. 11-13), it is suggested that the Rankine or Coulomb solution may be better than the graphical methods for surcharges located within the Rankine wedge defined by the angle  $\rho$  (Slope of  $AC$  shown on Fig. 11-7a).

If the surcharge is located within this zone, simply convert the surcharge to a vertical load, divide by the distance  $BC$  (see also the figure on Table 11-7), and treat the result as a surcharge  $q$ .

If the surcharge lies outside the distance  $BC$  the best solution is generally the Coulomb or Rankine method plus the contribution from using the Theory of Elasticity of Sec. 11-13.

A special case of backfill surcharge is one located a distance  $d$  from the back face of the wall. Motta (1994) has produced a closed-form solution but the equations are difficult. They have been programmed in subroutine MOTTAKA in program FFACTOR as option 9; data are input using screen prompts. All the values in MOTTAKA have been previously used (i.e., consistent notation).

## 11-12 GRAPHICAL AND COMPUTER SOLUTIONS FOR LATERAL EARTH PRESSURE

There are graphical solutions for estimating lateral forces when the backfill is irregular-shaped or loads are concentrated. Neither of these cases is consistent with the Rankine or Coulomb theories. Among the several solutions are Culmann's (ca. 1886), the trial wedge method (ca. 1877), and the logarithmic spiral.

An analytical solution based on the Theory of Elasticity can also be used. This is particularly suited for computer use.

The Culmann and trial wedge methods are very similar except for the general orientation of the force polygons. Both methods rely on computing the known forces on a trial wedge, which include any external load on the backfill, the weight of the trial wedge, and the shear force on the tentative (or trial) rupture surface, and, from known slopes of the unknown wall force vector  $P_a$  (or  $P_p$ ) and the unknown resultant force  $R$  on the rupture surface, plotting